

# Sources of uncertainty in direct seismological measurements of the solar helium abundance

A. G. Kosovichev,<sup>1,2,3,4</sup> J. Christensen-Dalsgaard,<sup>1,5</sup> W. Däppen,<sup>1,2,6,7</sup>  
W. A. Dziembowski,<sup>1,2,8</sup> D. O. Gough<sup>1,2,4,9,10,11</sup> and M. J. Thompson<sup>1,10</sup>

<sup>1</sup>*Institute for Theoretical Physics, University of California, Santa Barbara, CA 93106, USA*

<sup>2</sup>*Institute of Astronomy, Madingley Road, Cambridge CB3 0HA*

<sup>3</sup>*Crimean Astrophysical Observatory, p/o Nauchny, Crimea 334413, Ukraine*

<sup>4</sup>*Center for Space Science and Astrophysics, Stanford University, CA 94305, USA*

<sup>5</sup>*Institut for Fysik og Astronomi, Aarhus Universitet, DK 8000, Aarhus C, Denmark*

<sup>6</sup>*Departments of Physics and Astronomy, University of Southern California, CA 90089-1372, USA*

<sup>7</sup>*Institut für Astronomie, Universität Wien, Vienna A-1180, Austria*

<sup>8</sup>*N. Copernicus Astronomical Center, ul. Bartycka Nr 18, Warsaw, Poland*

<sup>9</sup>*Department of Applied Mathematics and Theoretical Physics, University of Cambridge, Silver Street, Cambridge CB3 9EW*

<sup>10</sup>*Astronomy Unit, Queen Mary and Westfield College, Mile End Road, London E1 4NS*

<sup>11</sup>*Joint Institute for Laboratory Astrophysics, University of Colorado and National Institute of Standards and Technology, Boulder, CO 80309, USA*

Accepted 1992 May 27. Received 1992 May 27; in original form 1992 February 25

## ABSTRACT

The methods by which Däppen et al. and Dziembowski, Pamyatnykh & Sienkiewicz recently obtained discrepant estimates of the helium abundance in the solar convection zone are compared. The aim of the investigation reported in this paper is to identify the main source of the discrepancy. Using as proxy data eigenfrequencies of a set of modes of a theoretical solar model, computed with the same physics as were the frequencies of a reference model with which these data are compared, the two methods yield similar results. Thus we ascertain that the principal source of the discrepancy is not in the inversions themselves, which yield essentially a measure of the variation of the adiabatic exponent  $\gamma$  of the material in the He II ionization zone. Instead it is in the approximations adopted in the treatment of heavy elements in the equation of state used to relate the variation of  $\gamma$  to chemical composition. We obtain acceptably consistent results when inverting solar data by two methods using the same equation of state. We attempt to identify the likely residual sources of uncertainty.

**Key words:** Sun: abundances – Sun: interior – Sun: oscillations.

## 1 INTRODUCTION

Direct seismological measurements of the helium abundance in the solar convection zone are obtained from the variation of the adiabatic compressibility of the stellar material in the second helium ionization zone. What is actually measured is basically a relation between pressure  $p$ , density  $\rho$  and the adiabatic exponent  $\gamma = (\partial \ln p / \partial \ln \rho)_s$ , the partial derivative being taken at constant specific entropy  $s$ . Because turbulent Reynolds stresses are small well beneath the upper super-adiabatic boundary layer in the convection zone, the additional constraint imposed by the hydrostatic equation relates the variation of pressure directly to that of density. The seismic data can thus be expressed in terms of  $\gamma$  and  $\rho$  alone,

from which it is possible to isolate the variation of  $\gamma$ , which itself depends on chemical composition. It is sensitive predominantly to the relative abundances  $X$  and  $Y$  of hydrogen and helium, although, to a lesser extent, it depends also on the abundances of the heavier elements. The greatest variation of  $\gamma$  is produced by the ionization of hydrogen and the first ionization of helium, which one might therefore think are the best diagnostics of  $Y$ . However, these ionizations occur in the poorly understood convective boundary layer in which the stratification is ill-determined. It is only deeper down, in the second helium ionization zone, where the stratification is very close to being isentropic and the convective velocities are small, that we can be sure of the equation governing the hydrostatic balance.

Early attempts to determine  $Y$  in the He II ionization zone (Däppen & Gough 1986; Däppen, Gough & Thompson 1988a) used a first-order asymptotic theory of stellar oscillations to estimate the variation of  $\gamma$  from the derivative of the square of the sound speed (Gough 1984a). It was found that the diagnostic employed was rather insensitive to the value of  $Y$ , and therefore that the measurement (which yielded  $Y=0.233\pm 0.003$ ) may not be reliable. Consequently, a more sophisticated approach was adopted, in which information contained in the phase of the oscillation eigenfunction in the He II ionization zone, ignored by previous asymptotic analyses, was automatically taken into account (Däppen et al. 1991). The method was based on a linearization of the difference between the Sun and a reference solar model, the variations of  $\gamma$  being expressed in terms of an optimally localized average of  $Y$ , in the sense of Backus & Gilbert (1968, 1970), via the equation of state applied to the reference model. The result, originally reported by Gough & Toomre (1990), was  $Y=0.268\pm 0.01$ .

Soon afterwards, Dziembowski, Pamyatnykh & Sienkiewicz (1991), using a regularized least-squares fitting procedure (cf. Phillips 1962; Tikhonov & Arsenin 1977), obtained  $Y=0.234\pm 0.005$ , and Christensen-Dalsgaard & Pérez Hernández (1991) and Vorontsov, Baturin & Pamyatnykh (1991), by calibrating asymptotic phases of solar oscillations against those of a sequence of theoretical models, obtained  $Y=0.25$ , with a formal error of  $\pm 0.01$  in the latter case.

The wide discrepancies between these results demand explanation. Accordingly we have carried out a series of tests. We have concentrated only on the direct inversion methods, principally because they are aimed more explicitly at isolating the value of  $Y$  from other properties of the Sun. Although we have succeeded in understanding much of the difference between the results of the two published inversions, our understanding of the physics of the Sun is not yet adequate for us to offer a significantly more reliable estimate of  $Y$ . Nevertheless, in view of the recent appearance in the literature of the disparate determinations without any discussion of the possible origins of the disparities, we regard it as useful to report now on our findings.

We emphasize that we are attempting to make a direct measurement of the helium abundance in the convection zone now, and that as a result of gravitational settling against diffusion this value is likely to be smaller than the primeval value (e.g. Proffitt & Michaud 1991).

## 2 THE METHODS OF INVERSION

Both inversions (Däppen et al. 1991; Dziembowski et al. 1991) start, in principle, from the linearized equation (cf. Gough & Thompson 1992)

$$\frac{\delta\nu_i}{\nu_i} = \int_0^{\Xi} \left[ K_{f,\gamma}^{(i)} \frac{\delta f}{f} + K_{\gamma,f}^{(i)} \frac{\delta\gamma}{\gamma} \right] dx \quad (1)$$

for differences  $\delta\nu_i$  between the observed cyclic frequencies of oscillation of the Sun and the corresponding multiplet cyclic eigenfrequencies  $\nu_i$  of a spherically symmetric reference solar model. The  $\delta\nu_i$  are expressed in terms of both the difference  $\delta f$ , at fixed geometrical radius  $r$ , between the spherically symmetric component of the structure of the Sun and the structure  $f(x)$  of the model, and the difference  $\delta\gamma$

in the adiabatic exponent  $\gamma$ . Here,  $f$  is either density or the function  $u=p/\rho$  which is proportional to the square of the sound speed; the independent variable  $x$  is either  $r$  or acoustical radius  $\tau = \int c^{-1} dr$ , where  $c$  is adiabatic sound speed, each measured in units of its value at the photosphere;  $\Xi$  is the value of  $x$  at the surface of the reference solar model, which is near the temperature minimum. With a knowledge of the abundances  $X_k(x)$  of chemical elements  $k$  in the reference model, the equation of state  $\gamma = \gamma(p, \rho, X_k)$  can be used to transform equation (1) into

$$\frac{\delta\nu_i}{\nu_i} = \int_0^{\Xi} \left[ K_{f,\gamma}^{(i)} \frac{\delta f}{f} + K_{Y,f}^{(i)} \delta Y \right] dx, \quad (2)$$

where  $Y \equiv X_4$  is the abundance of  ${}^4\text{He}$ . Here we do not consider variations in abundances  $X_k$  other than in  $Y \equiv X_4$  and  $X \equiv X_1 \equiv 1 - Y - Z$ . At this stage  $\delta Y$  is formally a function of  $x$ , since we have not yet used the information that the convection zone is well mixed. The label  $i = (n, l)$  identifies the multiplet, where  $n$  is order and  $l$  is degree.

In practice, probably the major deficiency in equation (2) is in the outer layers of the model, in and above the super-adiabatic convective boundary layer, where the physics is poorly understood. Consequently, it is incumbent upon us to seek a measure of  $Y$  that is insensitive to conditions in that region. This is carried out by recognizing that, if the errors in the surface layers of the model are not propagated (via the oscillation eigenfunctions, upon which the kernels  $K_{f,\gamma}^{(i)}$  and  $K_{Y,f}^{(i)}$  depend) deep into the interior, then the errors in the contribution to the theoretical eigenfrequencies  $\nu_i$  can largely be written as model-dependent functions of frequency divided by the inertia (or energy)  $E_i$  of the mode normalized to unit vertical displacement (or velocity) amplitude in the region where the uncertainty is greatest. Accordingly, both inversion methods essentially subtract from the data  $\delta\nu_i/\nu_i$  a quantity  $F(\nu_i)/E_i$ , where  $F$  is an unknown function of frequency. In both cases,  $F$  is expressed as a truncated series of Legendre polynomials  $P_\lambda(\mu_i)$  with unknown coefficients  $a_\lambda$  ( $0 \leq \lambda \leq \Lambda$ ) that are independent of  $\nu_i$ ; here

$$\mu_i = \frac{2\nu_i - (\nu_s + \nu_m)}{\nu_s - \nu_m}, \quad (3)$$

where  $\nu_m$  and  $\nu_s$  are respectively the smallest and largest frequencies in the data used. [In their earlier paper, Dziembowski, Pamyatnykh & Sienkiewicz (1990) used a power series in  $\nu$ , but the difference is only one of numerical convenience.]

The procedure adopted by Däppen et al. (1991), which we call method 1, was to construct appropriate linear combinations

$$\sum_i c_i \nu_i^{-1} \delta\nu_i \quad (4)$$

of the data from coefficients  $c_i(x_0)$  designed to make unimodular  $Y$ -averaging kernels

$$A_{Y,f}(x; x_0) = \sum c_i(x_0) K_{Y,f}^{(i)}(x) \quad (5)$$

well localized about a chosen location  $x = x_0$ , and the corresponding  $f$ -averaging kernels

$$A_{f,\gamma}(x; x_0) = \sum c_i(x_0) K_{f,\gamma}^{(i)}(x) \quad (6)$$

small everywhere, subject to the data combination (4) being invariant under the transformation

$$\delta\nu_i \rightarrow \delta\nu_i - E_i^{-1} F(\nu_i), \quad (7)$$

where

$$F(\nu_i) = \sum_{\lambda=0}^{\Lambda} a_{\lambda} P_{\lambda}(\mu_i) \quad (8)$$

for all constants  $a_{\lambda}$ , and the localization of  $A_{Y,f}$  is moderated by the requirement that the combination (4) is not excessively sensitive to errors in the data. This is achieved by minimizing, for chosen trade-off parameters  $\alpha_1$  and  $\beta$  and for a given value  $\Lambda_1$  of  $\Lambda$ , the quantity

$$\int_0^{\Xi} [(A_{Y,f})^2 J(x, x_0) + \beta(A_{f,Y})^2] dx + \alpha_1 \sum_i c_i^2 \sigma_i^2, \quad (9)$$

subject to  $\int_0^{\Xi} A_{Y,f} dx = 1$ , and the  $\Lambda_1 + 1$  additional constraints

$$\sum_i c_i P_{\lambda}(\mu_i) / E_i = 0; \quad \lambda = 0, 1, 2, \dots, \Lambda_1. \quad (10)$$

The quantities  $\sigma_i$  are the observers' estimates of the standard relative errors in the frequencies  $\nu_i$ , which are assumed to be independent. The function  $J(x, x_0)$  is zero at  $x = x_0$ , and increases as  $x$  both decreases and increases away from  $x_0$ . Däppen et al. (1991) chose  $J = (x - x_0)^2$ , as do we in the inversions reported here. Thus the combination (4) represents essentially an average  $\overline{\delta Y}$  of  $\delta Y$ , given by

$$\begin{aligned} \overline{\delta Y}(x_0) &\equiv \int_0^{\Xi} A_{Y,f}(x; x_0) \delta Y(x) dx + \int_0^{\Xi} A_{f,Y}(x; x_0) \frac{\delta f(x)}{f(x)} dx \\ &= \sum_i c_i \frac{\delta\nu_i}{\nu_i} \end{aligned} \quad (11)$$

in the vicinity of  $x = x_0$ , but is contaminated by a small contribution from  $\delta f$ . In principle, by varying  $x_0$  one can attempt to determine averages of  $\delta Y$  that are concentrated near different locations  $x_0$ , and so test the inversion. In practice, however, it is possible to localize  $K_{Y,f}$  only in and above the He II ionization zone. By interchanging  $A_{Y,f}$  and  $A_{f,Y}$  in equation (9) one can similarly sample the function  $\delta f/f$  (see Däppen et al. 1991).

The procedure of Dziembowski et al. (1991), which we call method 2, is described by Dziembowski et al. (1990). It is accepted at the outset that  $\delta Y$  is independent of  $x$ , at least in the ionization zones where  $\gamma$  varies, and hence equation (2) is rewritten

$$\begin{aligned} \delta\nu_i &= \left[ \int_0^{\Xi} K_{f,Y}^{(i)} \frac{\delta f}{f} dx + \delta Y \int_0^{\Xi} K_{Y,f}^{(i)} dx + E_i^{-1} F(\nu_i) \right] \nu_i \\ &\equiv \Delta_i(\delta f, \delta Y, a_{\lambda}), \end{aligned} \quad (12)$$

in which we have explicitly accounted for the unknown contribution from the surface layers by the last term in square brackets in which  $F(\nu_i)$  is again taken to be of the form (8), but now with  $\Lambda = \Lambda_2$ . The function  $\delta f/f$  is represented as a superposition of cubic splines, and the spline coefficients, together with  $\delta Y$  and  $a_{\lambda}$  ( $\lambda = 0, 1, 2, \dots, \Lambda_2$ ) in

the expansion (8) of  $F$ , are determined by minimizing, for some trade-off parameter  $\alpha_2$ , the quantity

$$\mathcal{E} \equiv \sum_i \left( \frac{\delta\nu_i - \Delta_i}{\sigma_i \nu_i} \right)^2 + \alpha_2 \int_0^{\Xi} \left( x \frac{d}{dx} \frac{\delta f}{f} \right)^2 dx. \quad (13)$$

Thus in this case the correction  $\delta Y$  to the helium abundance is determined simultaneously with the structure correction  $\delta f/f$ . It is given, once again, as a linear combination (4) of frequency differences, though now there is but a single set of coefficients  $c_i$  because  $\delta Y$  is assumed to be independent of  $x$ . Thus for this method too, averaging kernels  $A_{Y,f}$  and  $A_{f,Y}$  exist (cf. Thompson 1991), as defined by equations (5) and (6). In this paper we regard just this procedure for inverting the linearized constraints (2) as method 2. Dziembowski et al. (1991) additionally applied a non-linear adjustment to their results, which we discuss in Section 4.5.

### 3 PREVIOUS INVERSIONS AND TESTS

In this section we summarize briefly the inversions that have been published and the tests of them that have been carried out. We must do this in order to acquire an appreciation of how the differences between the published results might be explained.

#### 3.1 Solar data

For method 1, a homogeneous data set taken from observations carried out in 1986 by Libbrecht, Woodard & Kaufman (1990) was used. The modes observed had degrees in the range 4–1860. Däppen et al. (1991) selected only those modes satisfying  $l \leq 140$  and  $1500 \leq \nu \leq 3000$   $\mu\text{Hz}$ ; the reason for applying upper limits to both  $l$  and  $\nu$  was to protect the determination from inaccurate representation of modes whose frequencies are more strongly influenced by the very uncertain outer layers of the Sun, particularly the upper convective boundary layer. The resulting data set contained  $I = 598$  modes; we shall refer to it as  $\mathcal{D}$ . The rms error associated with the measured frequencies in  $\mathcal{D}$  was 0.04  $\mu\text{Hz}$ . Dziembowski et al. (1991) chose sets of modes from the compilation by Libbrecht et al. (1990) with degrees up to various upper limits  $l_{\max}$ , over the entire available frequency range. These data included some modes obtained by different techniques and at different times; thus the sets were not homogeneous.

#### 3.2 Equation of state

An important step in any seismic procedure for determining composition is relating macroscopic thermodynamical variables to chemical abundances. This requires the use of an equation of state, and evidently the accuracy to which one can determine  $Y$  is limited by the accuracy to which the equation of state is known. Although both published inversions had utilized tables of the MHD equation of state (Hummer & Mihalas 1988; Mihalas, Däppen & Hummer 1988; Däppen et al. 1988b), the versions were somewhat different. Däppen et al. (1991) used reference models from Christensen-Dalsgaard, Gough & Thompson (1991) which had been computed using some early tables for a mixture of H, He and of heavy elements represented by two species: O and Fe in the proportion 23:2. The ions of the heavy

elements were assumed to be always in their ground states. Dziembowski et al. (1991), on the other hand, used tables on a finer grid that had originally been prepared for the inversions of Däppen et al. (1988a). For these, all the heavy elements had been represented by only a single species, O. However, full MHD partition functions of all excited states were included. The restrictions in both versions of the equation of state were dictated by the limited availability of computer time. Throughout this paper we shall refer to these versions as MHD1 and MHD2, respectively. For the purpose of relating  $\delta\gamma$  to  $\delta Y$  in constructing the kernels  $K_{f,Y}$  and  $K_{Y,f}$ , it is necessary to know the partial derivatives of  $\gamma$  with respect to  $Y$  and two independent thermodynamic variables. These were not included in the original tables of MHD1, and therefore both groups used the values from the tables of MHD2. Thus the kernels computed by Däppen et al. (1991) were not strictly consistent with the reference model. At that time the details of the description of the heavy elements were believed not to be significant for determining  $\gamma$  and its derivatives in the He II ionization zone.

### 3.3 Previous tests for the procedures

All the inversions reported explicitly by Däppen et al. (1991) and Dziembowski et al. (1991) were carried out with the structure function  $f=u$ . Däppen et al. (1991) tested their procedure with artificial data; eigenfrequencies of a solar model, different from the reference, were used in place of solar data, with a view to inferring the structure and the helium abundance in the convection zone of the proxy Sun. The same mode set was used for the test as for the solar inversion, and it was assumed that standard errors in the data were the same as those quoted by Libbrecht et al. (1990). Inversions were carried out for different values of the trade-off parameter  $\alpha_1$ , in each case choosing  $\beta$  to render the estimated contamination from  $\delta f$  equal to the expected contribution from the data errors; the resulting  $Y$  was essentially independent of  $\alpha_1$  for  $\alpha_1 \geq 100$ . Moreover, the inferred  $Y$  depended only weakly on  $\Lambda_1$ , presumably because the optimal averaging kernels  $A_{Y,f}$  were small in the uncertain outer layers of the model. The numerical integrations were carried out by finite differences, using a finite non-uniform mesh adequate to resolve all the variations in the integrals. Däppen et al. also modified the proxy data to take some account of Reynolds stresses and non-adiabatic processes in the outer layers, yet retaining the simple adiabatic eigenfrequencies and eigenfunctions of the reference model for the inversion, and again found no significant influence on the value of  $Y$  inferred. Two reference models (models 2 and 4 in Table 1), both taken from Christensen-Dalsgaard et al. (1991) and with  $Y$  differing by 0.035, were used for the inversions, to test the validity of the linear approximation (2). In both cases the inferred  $Y$  agreed with the actual value within the formal errors of the inversion, which were about  $\pm 0.003$ . However, that was not quite the case for the solar inversions, which is why a larger uncertainty was quoted for the solar  $Y$ .

Dziembowski et al. (1990) had reported on tests with artificial data in their first paper. They too had investigated the influence of  $\Lambda_2$  and  $\alpha_2$  on the results. As  $\Lambda_2$  is increased from zero the inversion changes, and stabilizes for  $\Lambda_2 \geq 15$ ; moreover, the differences between the data and the inferred

frequencies of the proxy Sun are diminished. The suppression of unreal small-scale structure in the inferred  $\delta \ln f$  is achieved partly by the choice of the number of splines in the representation and partly by the regularization parameter  $\alpha_2$ . Although Dziembowski et al. (1990) found  $\alpha_2 \approx 50$ , with 20 or 30 splines, to be an acceptable trade-off between error magnification and resolution of  $\delta \ln f$ , the value of  $Y$  inferred was best when  $\alpha_2 = 0$ . This is presumably because spline knots were equally spaced in  $r$ , which was quite inadequate to resolve the He II ionization zone.

In their subsequent paper, Dziembowski et al. (1991) used acoustical radius  $\tau$  as the independent variable, again spacing the spline knots uniformly, which resolves the outer layers more finely. No direct test with artificial data was carried out, though five different reference models were used to invert the solar data. Values of  $Y$  varying from 0.238 to 0.254 were obtained, the disparity being interpreted as a result of the breakdown of the validity of the linearization from which equations (2) and (12) were derived. Under the assumption that the true relation can be obtained by adding to equation (12) a term quadratic in the estimate  $\bar{\delta Y}$  of  $\delta Y$  obtained by minimizing  $\mathcal{E}$ , Dziembowski et al. fitted inversions from four of their reference models to the formula

$$\delta Y = \bar{\delta Y} - C(\bar{\delta Y})^2, \quad (14)$$

where  $C$  was a constant whose value lay between 3.7 and 4.0, and  $\delta Y$  was the presumed actual difference between the solar  $Y$  and the  $Y$  of the reference model. They thereby deduced a solar  $Y$  somewhat lower than the linear estimates. Dziembowski et al. also tested the sensitivity of the inversions to the mode set employed, by varying  $l_{\max}$ ; they found that the results were stable for  $l_{\max} \geq 120$ , concluding from this that they had successfully eliminated the influence of the uncertain outer layers of the Sun by their use of the function  $F(\nu)$ . Moreover, they found that the inferred  $Y$  was stable for  $\Lambda_2 \geq 20$ .

Additional tests, not reported in the papers, had been carried out before the collaborative investigation summarized below was begun. In particular, Dziembowski et al. had considered the ability of  $F(\nu)$  to eliminate the influence of the surface layers by artificially setting  $K_{\gamma,u} = 0$  in equation (1) in and above the H ionization zone; they found no significant change in the inferred  $\delta Y$ . Däppen et al. found that replacing  $u$  by  $\rho$  for the structure function  $f$  also made no significant difference to  $Y$ . Moreover, they found that for inferring  $Y$  there is no significant difference between using  $r$  and  $\tau$  as independent variable; the resolution of the mesh used for the numerical computations was in both cases quite adequate. This conclusion does not conflict with the superficially contradictory statement made by Dziembowski et al. (1990); 40 splines were centred about points uniformly distributed with respect to the independent variable in method 2, and that provides inadequate resolution of the structure of the outer layers when the independent variable is  $r$ . However, using solar data, the value inferred for  $Y$  was changed by only 0.004 at fixed  $\alpha_2$  when  $r$  was used instead of  $\tau$ .

## 4 SOURCES OF DISPARITY

It is evident from the preceding discussion that there were various quite obvious differences between the procedures that had been carried out to obtain the two published inver-

sions for  $Y$ . We here report the results of our attempts to assess which are the most likely to have contributed substantially to the discrepancy between the conclusions. To this end we have carried out tests to compare the two methods. In addition, we have used an independently written program to invert the constraints (12); it is essentially the program used by Gough & Kosovichev (1988), with the regularization integral modified to be consistent with equation (13).

Most of our tests have been carried out using artificial solar data. These data were obtained as adiabatic eigenfrequencies of theoretical proxy solar models. The stratification of those models was obtained on a mesh suitable for computing the oscillation eigenfunctions by taking  $\rho(r)$  and the surface pressure from models listed in table 4 of Christensen-Dalsgaard et al. (1991), and computing  $p(r)$  by integrating the hydrostatic equations inwards using a centred difference scheme of second-order accuracy. The adiabatic exponent  $\gamma$  and its partial derivatives with respect to  $\rho$ ,  $p$  and  $Y$  were then computed with various versions of the equation of state; in carrying out this computation the helium abundance  $Y(r)$  was either that of the original model, or was taken from a different model. Two of those models, each with its own  $Y(r)$ , were also used as our reference models. The salient characteristics of the models are summarized in Table 1.

**Table 1.** Solar models.

Model	Opacity	$A$	Energy generation	Evolved or static	$Y_0$	$d_b/R$
2	CT	0	FCZ	E	0.2371	0.2851
4	LAOL	0	P	E	0.2724	0.2668
7	CT	-0.02	P	S	0.2320	0.2786
10	CT	0.1	P	S	0.2452	0.3013
13	LAOL	0.1	P	S	0.2850	0.2857
15	LAOL	0.2	P	S	0.2939	0.3055
R	LAOL	0	P	E	0.2689	0.273
H	CT	0	P	S	0.2803	0.2118

Solar models 2–15 are those of Christensen-Dalsgaard et al. (1991), with corresponding identification numbers, model R is model 3 of Dziembowski et al. (1991) and model H is a chemically homogeneous model in thermal balance. All have the solar mass  $M = 1.989 \times 10^{33}$  g, radius  $R = 6.960 \times 10^{10}$  cm and, except for model H, the solar luminosity  $L = 3.845 \times 10^{33}$  erg s $^{-1}$ . All models have  $Z = 0.0200$ , except model R which has  $Z = 0.0195$ , and all were computed with atmospheres obtained from the temperature–optical depth relation of the Harvard–Smithsonian Reference Atmosphere (Gingerich et al. 1971). CT refers to the opacity tables of Cox & Tabor (1976), LAOL to the Los Alamos Opacity Library (Huebner et al. 1977)<sup>a</sup>; FCZ denotes nuclear reaction parameters from Fowler, Caughlan & Zimmerman (1975), P the parameters of Parker (1986) and Bahcall & Ulrich (1988). The parameter  $A$  is the logarithm (to base 10) of an amplitude factor determining a quantity by which opacity is augmented in the temperature range  $1 \times 10^6$ – $4 \times 10^6$  K, in the manner defined explicitly by Christensen-Dalsgaard et al. (1991). E denotes that the model has been evolved from a chemically homogeneous zero-age main-sequence state; S denotes a model in thermal balance obtained by scaling the hydrogen abundance profile of a corresponding evolved model with  $A = 0$  by such a factor as to yield the correct luminosity.  $Y_0$  is the zero-age helium abundance, and  $d_b$  is the depth of the current convection zone.

<sup>a</sup>In all cases opacities were obtained by linear interpolation with respect to  $Y$  and by using two-dimensional stretched splines with respect to  $\log \rho$  and  $\log T$ .

The versions of the equation of state we have used are labelled MHD1–MHD5, and include those used for the previously published inversions. The characteristics of MHD1 and MHD2 were described in Section 3.2, though here we used new MHD1 tables computed on the finer grid of MHD2 and with consistent partial derivatives of  $\gamma$ . The effect of the grid size is discussed in Section 4.9. The remaining three versions, also computed on the finer grid, are described in Section 4.9 where, in addition, the effect of errors in the equation of state are discussed. Otherwise, all tests with artificial data consistently employed MHD5 for both the reference and the proxy models.

The tests we have carried out, and the conclusions that we have drawn from them, are set out below. The results are summarized in Table 2 and Figs 2–15. In most cases artificial data were used and, except where stated to the contrary, no errors were added to them. Unless stated otherwise, the inversions were of the frequencies in set  $\mathcal{D}$ , and the values of  $\sigma_i$  were taken to be those quoted by Libbrecht et al. (1990). The structure function  $f$  was taken to be  $u = p/\rho$  in all cases, and the independent variable  $x$  was the acoustical radius  $\tau$ . For brevity, where we quote a numerical value of  $Y$  in what follows, we refer to the constant value in the convection zone.

#### 4.1 Inversion procedures

Our first aim was simply to compare the two methods using the same reference models and the same artificial data sets. Moreover, the proxy models were computed with the same equation of state as the references. Inversions with respect to two reference models are recorded in rows 1 and 6–14 of Table 2. From those, and from all the others we have carried out, the inferred values  $\bar{Y}$  of  $Y$  were typically within 0.003 of the actual values. Thus we arrive at one of the principal conclusions of this investigation: if the reference model were truly a good, though not precise, representation of the Sun (in the sense that the physics were represented reliably, even though parameters such as  $Y$  were incorrect), and if our solution to the forward problem of determining the oscillation eigenfrequencies of the model were also a good representation of reality, for the purposes of determining  $Y$  there would be little to choose between the inversion methods, at least if accuracy were the sole criterion. In coming to this conclusion, it was necessary to choose trade-off parameters  $\alpha_1$ ,  $\beta$  and  $\Lambda_1$  in method 1, and  $\alpha_2$  and  $\Lambda_2$  in method 2; we discuss below how the choice was made, and how those parameters influence the inferences. It is pertinent here to report that, if in the least-squares inversion the regularization integral in equation (13) is replaced by that used by Gough & Kosovichev (1988), the resulting change in  $\bar{Y}$  is less than the difference between the inversions by least squares and by optimal averages. Consequently the precise choice of regularization integral is unimportant, at least when the physics is well represented. (We have found also that the precise choice of the integral is unimportant when solar data are used.)

The essential difference between the two inversion methods is best appreciated by inspecting the averaging kernels  $A_{Y,u}$  which weight the averages  $\bar{Y}$  of the inferred  $Y$ , and the kernels  $A_{u,Y}$  which provide an indication of how the inference is contaminated by the relative difference  $\delta \ln u$  in

**Table 2.** Summary of inversions: Inferences  $\bar{Y}$  of helium abundances of proxy solar models and the Sun.

No	Reference			Proxy or sun			Method 1		Method 2		
	Model	EQS	$Y_0$	Model	EQS	$Y_0$	$\delta Y$	$\bar{Y}$	$\Delta Y$	$\bar{Y}$	$\Delta Y$
1	2	5	0.2371	4'	5	0.2371	0	0.2347	-0.0024	0.2379	0.0008
2	2	5	0.2371	4	1	0.2724	0.0353	0.2487	-0.0237	0.2495	-0.0229
3	2	5	0.2371	4	2	0.2724	0.0353	0.2626	-0.0098	0.2664	-0.0060
4	2	5	0.2371	4	3	0.2724	0.0353	0.2715	-0.0009	0.2744	0.0020
5	2	5	0.2371	4	4	0.2724	0.0353	0.2661	-0.0061	0.2679	-0.0045
6	2	5	0.2371	4	5	0.2724	0.0353	0.2706	-0.0018	0.2756	0.0032
7	2	5	0.2371	7	5	0.2320	-0.0051	0.2319	-0.0001	0.2323	0.0003
8	2	5	0.2371	10	5	0.2452	0.0081	0.2451	-0.0001	0.2458	0.0006
9	2	5	0.2371	13	5	0.2850	0.0479	0.2855	0.0005	0.2859	0.0009
10	2	5	0.2371	15	5	0.2939	0.0568	0.2961	0.0022	0.2904	-0.0035
11	2	5	0.2371	H	5	0.2803	0.0432	0.2838	0.0029	0.2671	-0.0132
12	4	5	0.2724	2	5	0.2371	-0.0353	0.2357	-0.0014	0.2408	0.0037
13	4	5	0.2724	7	5	0.2320	-0.0404	0.2312	-0.0008	0.2328	0.0008
14	4	5	0.2724	10	5	0.2452	-0.0272	0.2419	-0.0033	0.2554	0.0102
15	2	1	0.2371	2	1'	0.2371	0	0.2336	-0.0035	0.2372	0.0001
16	2	1	0.2371	Sun				0.2516		0.2483	
17	2	2	0.2371	Sun				0.2331		0.2313	
18	2	3	0.2371	Sun				0.2268		0.2246	
19	2	4	0.2371	Sun				0.2318		0.2301	
20	2	5	0.2371	Sun				0.2256		0.2262	
21	2	5	0.2371	Sun*				0.2266		0.2263	
22	4	1	0.2724	Sun				0.2557		0.2555	
23	4	2	0.2724	Sun				0.2352		0.2420	
24	4	3	0.2724	Sun				0.2284		0.2344	
25	4	5	0.2724	Sun				0.2291		0.2368	
26	4	5	0.2724	Sun*				0.2299		0.2347	
27	R	2	0.2689	Sun						0.242	
28	R	2	0.2689	Sun†						0.237	
29	R	2	0.2689	Sun†§						0.276	

The model identifications refer to the models from which the frequencies were obtained; they are the same as in Table 1; model 4' has the density distribution of model 4 but the helium abundance distribution  $Y(r)$  of model 2. The identification 'Sun' refers to the frequencies of solar modes; except where indicated to the contrary, they are from the set  $\mathcal{D}$ , observed in 1986 by Libbrecht et al. (1990). EQS is the version of the MHD equation of state for computing  $\gamma$  and its derivatives. 1' refers to MHD1 obtained by interpolation in the coarser table (cf. Fig. 14).  $Y_0$  is the zero-age helium abundance, which is also the helium abundance in the convection zone of the model at the present time;  $\delta Y$  is the actual abundance difference between the proxy and reference models in the convection zone, and  $\Delta Y$  is the inversion error  $\bar{Y} - Y_0$ . In all cases inversions were carried out with the standard control parameters ( $\alpha_1 = 10^4$ ,  $\beta = 1$ ,  $\Lambda_1 = 3$  for method 1;  $\alpha_2 = 10^2$ ,  $\Lambda_2 = 13$  for method 2). In all cases but the last the standard errors quoted by Libbrecht et al. (1990) were used, leading to a formal error of 0.003 in  $\bar{Y}$  by both inversion methods.

Notes: \*the frequencies from the set  $\mathcal{D}$ , measured in 1988; †the extended data set containing all those modes measured by Libbrecht et al. in 1986 and by Jiménez et al. (1988); §the standard errors  $\sigma_i$  in these data have been assumed to be uniform and equal to the rms of the values used elsewhere; the formal error in  $\bar{Y}$  is 0.003.

the structures of the proxy model (or the Sun) and the reference. Some examples are illustrated in Fig. 1. A noticeable difference between the outcomes of the two methods is in the susceptibility to contamination of  $\bar{\delta Y}$  by  $\delta \ln u$ , which can be judged from the kernels  $A_{u,Y}$ . These kernels are all oscillatory with relatively small means, but the amplitudes of the kernels from the least-squares inversion are much greater

than those from optimal averaging. However, their means are rather less. Evidently, if  $\delta \ln u$  were smooth, as it tends to be between theoretical models computed with the same physics, then the contamination is small, particularly in the least-squares inversion. However, if in reality  $\delta \ln u$  varies as rapidly as  $A_{u,Y}$  in a region where  $A_{u,Y}$  is substantial, as it might in the ionization zones or near the base of the convec-

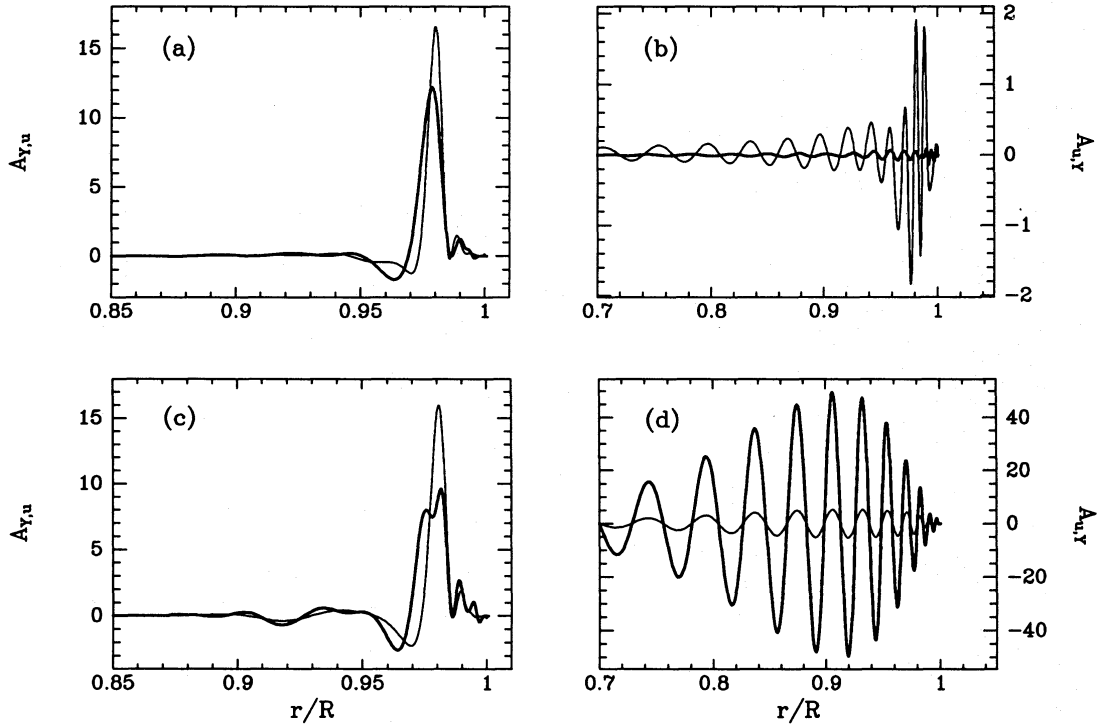


**Figure 1.** Averaging kernels of solar model 2 with MHD5 from the two methods of inversion: (a) and (b) are respectively the optimally localized  $Y$  and  $u$  averaging kernels  $A_{Y,u}$  and  $A_{u,Y}$  computed by method 1 with  $\alpha_1 = 10^4$ ,  $\Lambda_1 = 3$  and  $\beta = 1$  (thick curve),  $\beta = 10^{-3}$  (thin curve); (c) and (d) are corresponding kernels from least-squares inversions computed by method 2 with  $\alpha_2 = 10^2$  and  $\Lambda_2 = 13$  (thick curve),  $\Lambda_2 = 3$  (thin curve). The thick curves result from our standard control parameters. The abscissa is  $r/R$ , where  $R$  is the radius of the photosphere.

tion zone (see Fig. 11), then an erroneous inference of  $\delta Y$  is likely to result, and in that case it is the least-squares inversion that would be the more severely affected.

## 4.2 Regularization

The degree of regularization is determined principally in method 1 by the parameter  $\alpha_1$ , which explicitly moderates the error in  $\bar{Y}$  caused by errors in the data, and in method 2 by  $\alpha_2$ , which moderates the flatness of the inferred relative deviation  $\delta \ln u$ . Since helioseismology based on adiabatic motion depends solely on hydrostatic stratification, and the bulk compressibility of the medium, we first performed inversions of oscillation frequencies of a proxy model which differs from the reference only through the density distribution. Explicitly, we chose the density profile of model 2 for the reference and that from model 4 for the proxy;  $Y(r)$  was taken from model 2 in both cases, for the purposes of computing  $\gamma$  and its derivatives with MHD5. Thus  $\delta Y \equiv Y_{\text{proxy}} - Y_{\text{ref}} = 0$ . The results of the inversions are shown in Fig. 2 for various values of  $\alpha_j$  and  $\Lambda_j$  ( $j = 1, 2$ ). In the case of optimally localized averages it is also necessary to choose  $\beta$ . If  $\beta$  is too small, errors  $\delta f$  in  $f$  of the reference model contaminate the inversion too severely; if  $\beta$  is too large, the resulting excessive magnitudes of the coefficients  $c_i$  cause the inversion to be degraded by the errors in the data. Accordingly,  $\beta$  was chosen such that the magnitude of the estimated contamination due to  $\delta \ln u$  is the same as the potential contribution by data errors (more precisely, to satisfy equation 16), the latter being illustrated by the error bars about the inversions with  $\Lambda_1 = 3$ . For both methods the inferred value

$\overline{\delta Y}$  of  $\delta Y$  tends to improve with increasing  $\alpha_j$  and, when  $\alpha_j$  is large, is generally only quite weakly dependent on  $\Lambda_j$ . In all cases errors in the optimally localized averages were computed from  $\sigma_i$  and the coefficients  $c_i$ . Some were checked by inverting 100 different data sets obtained by adding Gaussian-distributed random errors with relative variance  $\sigma_i^2$  to the eigenfrequencies of the proxy model. The errors in the least-squares inversions were estimated from inversions of the data sets with added errors. Only at the largest value of  $\alpha_2$  is a divergence in the least-squares inversions with different values of  $\Lambda_2$  evident. That divergence rapidly becomes much more severe if  $\alpha_2$  is increased yet further. The results of the inversions with our standard regularization parameters (see Section 4.4) are listed in the first row of Table 2. It is noteworthy that the relative density difference  $\delta\rho/\rho$  between the proxy and reference models is not small, the density of the reference in the surface layers exceeding that of the proxy by a factor of about 2. Thus the exercise demonstrates that the inversions can quite successfully eliminate erroneous contributions to the eigenfrequencies arising from quite substantial errors in the reference model.

To demonstrate how the inversions depend on the control parameters when  $\delta Y \neq 0$ , we illustrate in Figs 3–8 inversions of model 4, using now the correct distribution of helium for that model. Once again the reference is model 2.

Fig. 3 is the analogue of Fig. 2(b), and shows a superficially similar convergence of method 2 with increasing  $\alpha_2$ , together with the divergence for the largest value considered. However, the value to which the inversions seem to converge is somewhat too high. The best inversions appear to occur for  $\alpha_2 \approx 10^2$ , with the largest value of  $\Lambda_2$ . The precision with

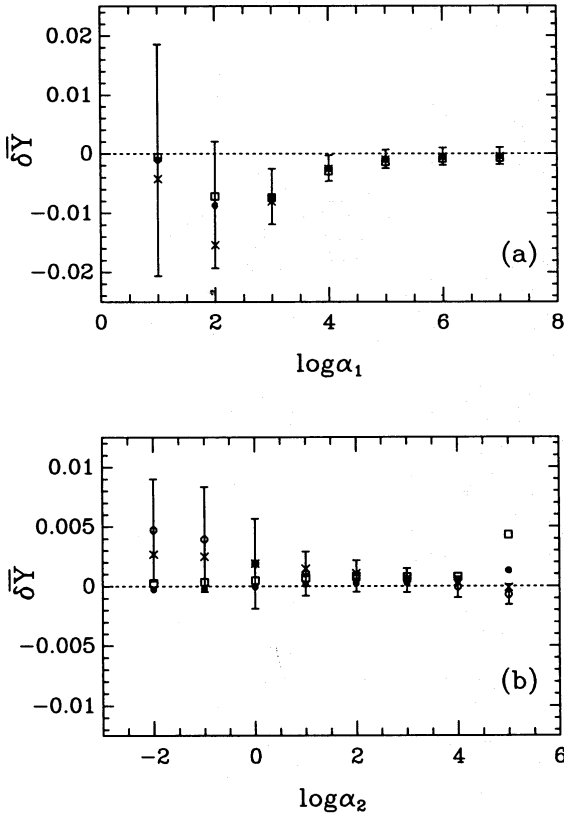


**Figure 2.** Inferred values  $\overline{\delta Y}$  of  $\delta Y$  for a sequence of inversions testing the influence of hydrostatic structure for different values of  $\alpha_i$  and  $\Lambda_j$ . Reference solar model: model 2 with MHD5; proxy solar model: density profile from model 4,  $Y_{\text{proxy}}(r) = Y_{\text{ref}}(r)$  which takes the value 0.2371 outside the energy generating core, MHD5 equation of state. (a) Optimal averaging inversions:  $F(\nu_i) = 0$  (squares);  $\Lambda_1 = 3$  (full circles with error bars);  $\Lambda_1 = 7$  (crosses). (b) Least-squares inversions:  $F(\nu_i) = 0$  (squares);  $\Lambda_2 = 3$  (full circles);  $\Lambda_2 = 7$  (crosses);  $\Lambda_2 = 13$  (open circles with error bars). Inversions for the standard control parameters are recorded in the first row of Table 2.

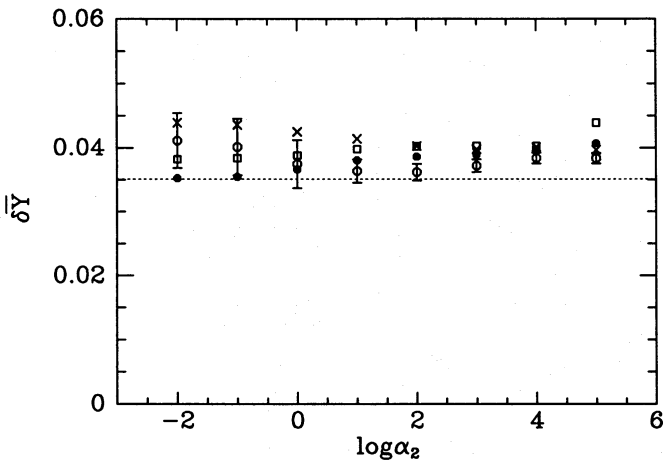


**Figure 3.** Inferred values  $\overline{\delta Y}$  of  $\delta Y$  as a function of  $\alpha_2$  for a sequence of test inversions by the least-squares technique. Reference solar model: model 2 with MHD5,  $Y = 0.2371$ ; proxy solar model: model 4 with MHD5,  $Y = 0.2724$ .  $F(\nu_i) = 0$  (squares),  $\Lambda_2 = 3$  (full circles),  $\Lambda_2 = 7$  (crosses),  $\Lambda_2 = 13$  (open circles with error bars). The dotted horizontal line indicates the true value of  $\delta Y$ .

which the frequencies of the proxy model are reproduced by the inversion is measured by

$$\chi^2 = \frac{\sum_i [(\delta \nu_i - \Delta_i) / (\nu_i \sigma_i)]^2}{\sum_i \sigma_i^{-2}}, \quad (15)$$

which is plotted against  $\alpha_2$  in Fig. 4. The value of

$$(I^{-1} \sum_i \sigma_i^{-2})^{-1/2}$$

for the  $I$  modes in  $\mathcal{D}$  is  $0.12 \mu\text{Hz}$ . As is typical of least-squares inversions,  $\chi^2$  increases quite slowly with  $\alpha_2$  when  $\alpha_2$  is small. It starts to rise rapidly only at the highest value of  $\alpha_2$  plotted, as the solution is falsified by too severe an imposition of the flatness constraint. Notice that  $\chi^2$  does not appear to decline to zero as  $\alpha_2 \rightarrow 0$ ; this is due to the fact that the spurious small-scale structures required in the solution to satisfy the frequency conditions (2) cannot be represented precisely by splines with a limited number of knots. The spline representation of the solution implicitly applies an additional smoothness constraint. In these, and all other inversions by method 2 reported in this paper, 40 spline knots, uniformly distributed with respect to  $\tau$ , have been used.

Some properties of optimally localized averaging are illustrated in the next two figures. Fig. 5 shows how  $\beta$  increases with  $\alpha_1$  in order to maintain the contamination of  $\overline{Y}$  by  $\delta \ln u$  at the level of the error in  $\overline{Y}$  potentially introduced by data errors. This balance is determined by the equation

$$\left( \int_0^T A_{u,Y} \overline{\delta \ln u} d\tau \right)^2 = \sum_i c_i^2 \sigma_i^2, \quad (16)$$

where  $T$  is the acoustical radius at the surface of the reference solar model and  $\overline{\delta \ln u}$  is itself obtained from an optimal-averaging inversion. For  $\alpha_1 > \alpha_c \approx 10^3$ , the precise value of  $\alpha_c$  depending on  $\Lambda_1$ , the solutions are stable and

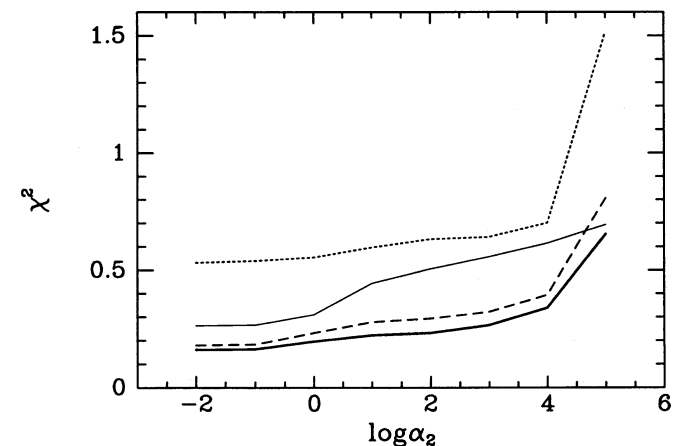


**Figure 4.** The mean-square deviation  $\chi^2$  for the sequences of test inversions by method 2 illustrated in Fig. 3, joined by dotted lines for the case  $F(\nu_i) = 0$ , dashed lines ( $\Lambda_2 = 3$ ), continuous thin lines ( $\Lambda_2 = 7$ ) and continuous thick lines ( $\Lambda_2 = 13$ ).



$\beta \propto \alpha_1$ . This is also the regime in which  $\bar{Y}$  hardly varies with  $\alpha_1$ , as can be seen in Fig. 6. At lower values of  $\alpha_1$ , where the widths of the optimal averaging kernels  $A_{Y,u}$  vary quite slowly with the influence of the data errors,  $\beta$  rises more steeply with  $\alpha_1$ . Fig. 5 is typical of all pairs of models we have used.

The dependence of the optimally localized averaging on  $\alpha_1$  is illustrated in Fig. 6. Within the range of the parameters considered, the inferred helium abundance improves with  $\alpha_1$  at fixed  $\Lambda_1$ ; not only does the influence of the data errors diminish, but also the value of  $\delta Y$  determined by the inversion improves as  $\alpha_1$  increases. This is as one would expect when proxy data computed by the same method as the reference frequencies are employed: because  $Y$  is constant throughout the envelopes of both the solar models, there is little to lose by permitting the widths of the  $Y$ -averaging kernels to increase as data errors are suppressed, at least if the rapidly varying superadiabatic boundary layer at the top

of the convection zone, in which the linearization might be suspect, is avoided. Moreover, the increase of  $\beta$  with  $\alpha_1$  also reduces contamination by structural differences between the two models. However, if  $\alpha_1$  is increased yet further (beyond about  $10^8$  for our artificial data, and about  $10^6$  for solar data), too little weight is given to the constraints (2) and the estimates of  $Y$  diverge.

### 4.3 Reduction of the influence of the surface layers

The purpose of the function  $F(\nu)$  is to account for the influence of the very uncertain outer layers of the convection zone, particularly on the least-squares inversion. It is evident from the asymptotic structure of the  $p$ -mode eigenfunctions (e.g. Unno et al. 1989; Gough 1992) that, near the surface of the star where  $L^2 c^2 / \omega^2 r^2 \ll 1$ ,  $L^2$  being either  $l(l+1)$  or  $(l+\frac{1}{2})^2$  and  $\omega$  being the angular frequency of the mode, the influence of the stratification of the background state of the star on the restoring force causing the acoustic oscillations is a function of frequency alone. This is largely the case also for the acoustic modulation of the turbulent fluxes of energy and, more importantly, momentum. The contribution to the (cyclic) frequency  $\nu_i$  is therefore of the form  $E_i^{-1} F(\nu_i)$  (e.g. Christensen-Dalsgaard 1991), and the introduction of a term of this form into equation (12) must eliminate the influence of a region  $\mathcal{R}$  immediately beneath the surface of the star. The form of that part of  $F$  that arises from the mean stratification in  $\mathcal{R}$  can be considered to contain a contribution coming from the evanescent region, together with a superposition of oscillatory functions whose ‘frequencies’ are roughly twice the acoustical depth of any contributing layer that lies beneath the upper turning point of the mode (Gough 1990). Therefore, as the number  $\Lambda + 1$  of terms in the representation (8) of  $F$  increases, higher frequency components are eliminated and not only is the influence of  $\mathcal{R}$  diminished, but also the depth of  $\mathcal{R}$  is increased. Consequently, a greater contribution from the He II ionization zone itself is removed, particularly from the eigenfrequencies of the low-degree modes for which the  $l$  dependence (which depends on  $1 - L^2 c^2 / \omega^2 r^2$ ) is small. The inversion relies to a greater and greater extent on the modes of high degree, whose lower turning points are not much deeper than the He II ionization zone and whose frequencies are not so well determined. (Note that  $\nu/L \approx 11 \mu\text{Hz}$  for modes whose lower turning points lie at  $r/R = 0.98$ , from which one deduces that the lower turning points of the least deeply penetrating modes in  $\mathcal{D}$ , for which  $\nu \approx 1.5 \text{ mHz}$  and  $l = 140$ , are within the He II ionization zone.) It is therefore essential not to adopt too great a value of  $\Lambda$ .

This property can be seen directly by inspecting the coefficients  $c_i$  of the data combination that determines  $\bar{\delta Y}$ . The increasing importance of high-degree modes, coupled with the increase in the subtlety of the combination of intermediate-degree modes, leads to an overall rise in the magnitudes of  $c_i$ . This explains the tendency for the uncertainty in the inversions by method 2, indicated by the error bars in Fig. 7, to be greater for the higher values of  $\Lambda_2$ . The contribution from the evanescent layers is inversely proportional to the inertia of the mode, and is thus approximately proportional to  $\nu^{2m+1}$ , where  $m \approx 3$  is the effective polytropic index of the envelope in the vicinity of the upper turning point (Gough 1990). Thus, as can be seen in Fig. 7, there is a

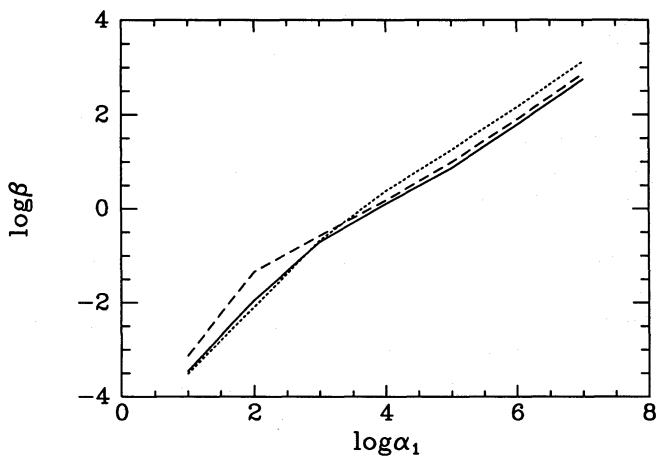


**Figure 5.** Regularization parameter  $\beta$  of optimally localized averaging chosen according to equation (16) such that the estimated contamination of  $\bar{Y}$  by the difference in the stratifications of the proxy (model 4) and the reference (model 2) is equal to the contribution propagated from the standard errors  $\sigma_i$ .  $F(\nu_i) = 0$  (joined by dotted lines),  $\Lambda_1 = 3$  (dashed lines),  $\Lambda_1 = 7$  (continuous lines).

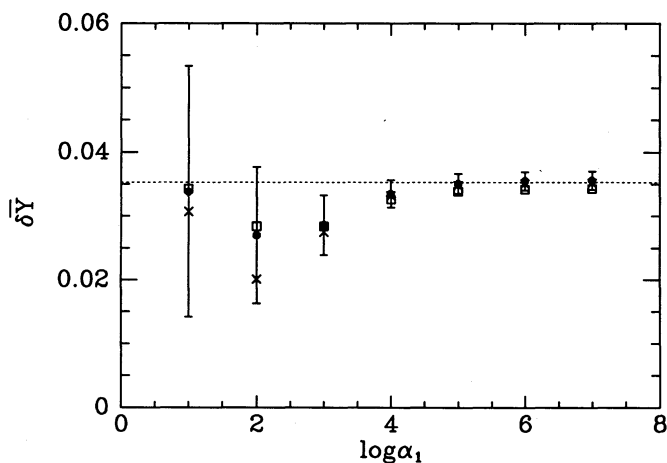


**Figure 6.** Analogue of Fig. 3, obtained by optimally localized averaging, with  $\beta$  determined by the balance (16), as illustrated in Fig. 5:  $F(\nu_i) = 0$  (squares),  $\Lambda_1 = 3$  (full circles with error bars),  $\Lambda_1 = 7$  (crosses). The dotted horizontal line indicates the true value of  $\delta Y$ .

stabilization of the inversion for  $\Lambda_2 \geq 7$  once the surface contribution is removed.

The impact of  $F$  on method 1 is considerably weaker, because, by their very construction, the optimal averaging kernels are constrained to be relatively small outside the He II ionization zone. In particular, they are smaller than the corresponding kernels of method 2 in the very surface layers, as can be seen in Fig. 1. Therefore the dependence of  $\overline{\delta Y}$  on  $\Lambda_1$ , which is illustrated in Fig. 8, is substantially weaker than it is for the least-squares method, as are the kernels from which it is constructed. However, the stabilization at higher  $\Lambda_1$ , this time for  $\Lambda_1 \geq 6$ , is again evident.

#### 4.4 On the choice of control parameters

In the light of the preceding discussion, we have selected  $\alpha_1 = 10^4$  for method 1. It can be seen from Figs 2(a) and 6 that it imposes the least amount of regularization in the range in which  $\overline{\delta Y}$  hardly depends on  $\alpha_1$ , and therefore permits

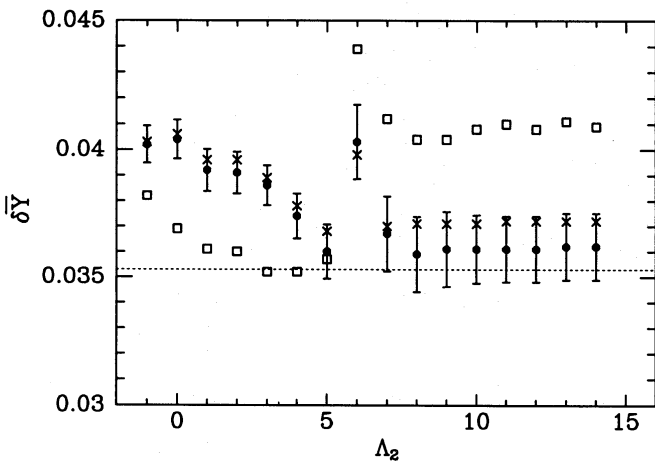


**Figure 7.** Dependence on  $\Lambda_2$  of test inversions by least squares. The proxy and reference models are the same as those used in Figs 3–6:  $\alpha_2 = 10^{-2}$  (open squares),  $\alpha_2 = 10^2$  (full circles with error bars),  $\alpha_2 = 10^6$  (crosses). Values plotted at  $\Lambda_2 = -1$  were obtained from inversions with  $F(\nu_i) = 0$ .

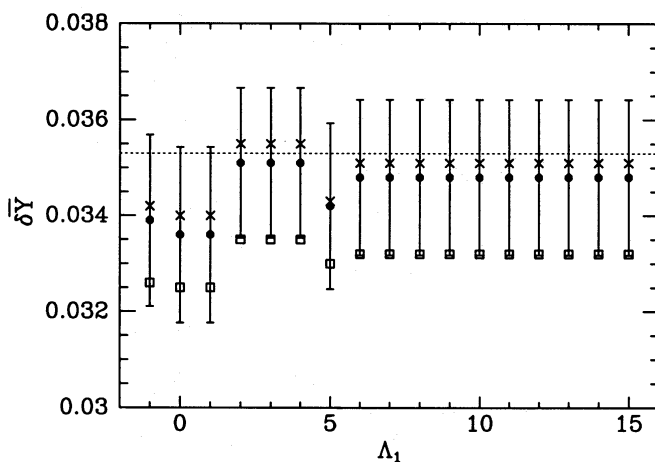


**Figure 8.** Analogue of Fig. 7, obtained by optimally localized averaging, with values of  $\beta$  plotted in Fig. 5:  $\alpha_1 = 10^4$  (open squares),  $\alpha_1 = 10^5$  (full circles with error bars),  $\alpha_1 = 10^6$  (crosses). The dotted horizontal line indicates the true value of  $\delta Y$ .

the greatest concentration of the  $Y$ -averaging kernel in that range. The corresponding value of  $\beta$ , which imposes the least constraint on the concentration of  $A_{Y,u}$  without contaminating the average  $\overline{\delta Y}$  more than the data errors, can be seen from Fig. 5 to be unity. Since the influence of  $F(\nu)$  is quite small, we have selected  $\Lambda_1 = 3$  as in the previous work (Däppen et al. 1991); higher values in principle degrade the power of the data yet, according to Fig. 8, seem to provide no improvement in the abundance determination.

It appears from Figs 2(b) and 3, and from a perusal of the inversions for  $\delta \ln u$ , that the optimal value of  $\alpha_2$  for method 2 is about  $10^2$ . This is sufficient to have removed most of the spurious small-scale structure in the inferred stratification difference  $\delta u/u$ , yet not so large as to have imposed excessive artificial flattening. This value is consistent with the value of 50 chosen by Dziembowski et al. (1990) using splines with knots regularly spaced in radius. The value employed (though it was not explicitly stated) in the subsequent estimation of the helium abundance using uniformly spaced spline knots with respect to acoustical radius (Dziembowski et al. 1991) was 10. The optimal choice of  $\Lambda_2$  is not so easy to ascertain. As is evident in Fig. 7, the inferred value of  $\delta Y$  is stable above  $\Lambda_2 = 7$ , which is rather lower than the value of 20 reported by Dziembowski et al. (1991). This is not surprising, because Dziembowski et al. needed to represent  $F(\nu)$  over a wider range of frequency than we do here. To correspond with the inversions of Dziembowski et al. (1991), we accordingly adopted the value  $\Lambda_2 = 13$  for most of our tests. We note, however, that the averaging kernels illustrated in Fig. 1 have much greater amplitudes for the larger value of  $\Lambda_2$ , and therefore must be more susceptible to systematic errors in the modelling.

We note, in passing, that the formal errors in the optimally localized averages can be reduced somewhat by choosing a function  $J$  in equation (9) that severely restricts  $A_{Y,f}$  only for  $x > x_0$ , permitting the averaging kernels to be broader within the convection zone beneath  $x_0$  where the chemical composition is presumed to be uniform. However, we do not advocate using such averages because they rely on the accuracy of the equation of state over a wider range of thermodynamic states than do the inversions presented in this paper.

Throughout the rest of the paper, we adopt as standard control parameters  $\alpha_1 = 10^4$ ,  $\beta = 1$ ,  $\Lambda_1 = 3$  with  $J = (\tau - \tau_0)^2$  for method 1, and  $\alpha_2 = 10^2$ ,  $\Lambda_2 = 13$  for method 2. For such values the formal error in  $\overline{Y}$ , based on the random data errors  $\sigma_i$ , is 0.003 for both methods. This is substantially less than the uncertainty of at least 0.02 evident in raw frequency comparisons of the kind considered by Guzik & Cox (1992), because the inversion procedures have successfully combined the data in such a way as to have eliminated the influence of errors outside the He II ionization zone. This was made possible by the use of a relatively large number of modes that sense the structure of the Sun in a variety of different ways.

#### 4.5 Linearity

We examine now the non-linear correction in equation (14). Its use by Dziembowski et al. (1991) represents a significant difference between the two procedures, because it caused a substantial reduction in the estimate of  $Y$ . In contrast, Däppen et al. (1991) had judged the correction to be neglig-

ible, because the results of inverting artificial data with respect to two different reference models had yielded essentially the same outcome. That conclusion is basically consistent with some earlier (unpublished) experiments with density inversions of mixed polytropes, having polytropic index  $m=3$  beneath some radius  $r=x_c R$ ,  $R$  being the radius of the solar photosphere, and  $m=3/2$  above; Cooper and Gough (see Cooper 1981; Gough 1984b) were able to obtain quite faithful linearized inversions when  $\delta\rho$  was in places as great as 40 per cent of the average of the densities of the two models.

Such linearity may not extend to the Sun. Indeed, in both investigations of  $\delta Y$  it was found that the disparities between inversions of solar data with respect to different reference models exceeded the errors anticipated. Dziembowski et al. (1991) noticed that the systematic trend was largely removed by the use of equation (14). Specifically, if it is assumed that  $\delta Y = \overline{\delta Y}$ , where  $\overline{\delta Y}$  is the linearized estimate obtained from the constraints (12), then from inversions of their reference models 2, 4, 5 and 6, which have the same atmosphere and are computed with the same equation of state, one finds that the rms deviation of the inferred  $Y$  from its mean value of 0.2464 is 0.0055. On the other hand, the rms deviation using equation (14) with  $C=4.12$  is only 0.0004, the mean this time being 0.2373. We note, in passing, that a non-linear correction of the form

$$\delta Y = \overline{\delta Y} - C|\overline{\delta Y}|^{3/2} \quad (17)$$

with  $C=1.21$  fits even better, the rms deviation of the inferred  $Y$  from its mean of 0.2345 being only 0.0002.

Moreover, the linear relation

$$\delta Y = 1.388 \overline{\delta Y} \quad (18)$$

also yields an almost constant value of  $Y$ , with the same deviation as is obtained from the use of equation (17), the mean inferred  $Y$  now being 0.2289.

In an attempt to locate the source of the difference between  $\delta Y$  and  $\overline{\delta Y}$  we have performed inversions of artificial data by the two methods, choosing both the reference and the proxy Sun from amongst models listed in Table 1. The results are illustrated in Fig. 9, in which  $\overline{\delta Y}$ , the abundance difference inferred by the linearized theory, is plotted against the actual difference  $\delta Y$ . Included, for comparison, are the non-linear relations (14) and (17). It is evident that the data fit  $\overline{\delta Y} = \delta Y$  quite well, and thereby confirm the validity of the linearization assumed in equations (1), (2) and (12). Notice that this is so despite the fact that the theoretical solar models do not even constitute a homogeneous set: they are based on different opacity tables, some of which are artificially modified, and different nuclear reaction rates and, furthermore, some are consistently evolved and some are not. Different equations of state were also used, but in all cases the same equation of state was used for the reference and the proxy models. We conclude, therefore, that the source of the disparity amongst the values of the solar helium abundance inferred by Däppen et al. (1991) and Dziembowski et al. (1991) from the linearized relations (2), using various reference models, cannot be reliably described by a simple non-linear relation such as is given by equation (14) or (17) between  $\delta Y$  and  $\overline{\delta Y}$ , presumed to arise from correc-

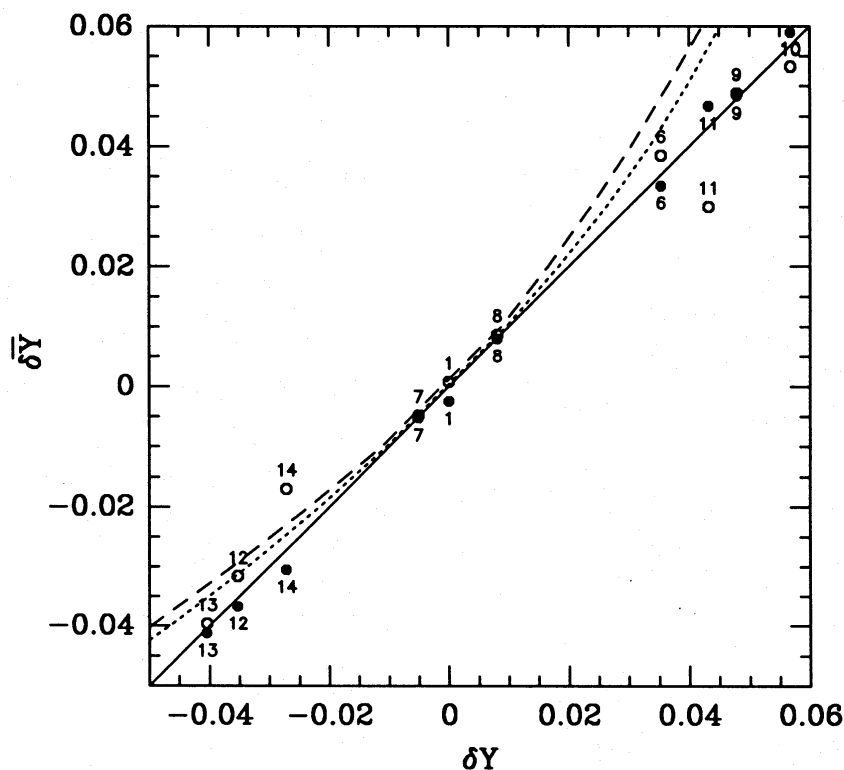


**Figure 9.** Inferred values  $\overline{\delta Y}$  of  $\delta Y$  obtained by optimally localized averaging (full circles) and least-squares inversions (open circles) of artificial data, plotted against the true  $\delta Y$ . The values are taken from Table 2 and are identified by row number in the figure; only those obtained with a reference computed with the same equation of state as that of the proxy are plotted. The dotted curve represents the non-linear relation (14) with  $C=4.12$ ; the dashed curve is relation (17) with  $C=1.21$ . The continuous line is  $\overline{\delta Y} = \delta Y$ .

tions to the constraints (2) from terms of higher order in the deviations  $\delta \ln u$  and  $\delta Y$ . There must be some other inconsistency between the reference frequencies and the solar data. We shall return to this point in Section 6.

#### 4.6 Influence of the atmosphere

Changing the atmospheric structure of the reference model might produce quite a profound influence both on the structure of the interior of that model when regarded as a function of  $r$  or  $\tau$  (Christensen-Dalsgaard 1988) and possibly, therefore, on the oscillation eigenfunctions too. Although the explicit modification is only to the very superficial layers, there is a significant reaction of the sound speed at constant  $r$  in the He II ionization zone (though at constant pressure or, equivalently, interior mass, the variation is substantially smaller). Its influence cannot therefore necessarily be eradicated solely by the extreme localization of the kernels of the reference model by method 1, nor can it be adequately represented by  $F(\nu)$ . One consequence is a slight modification to the inferred value of the linear correction  $\delta Y$ , as is evident from the calculations of Dziembowski et al. (1991), who compared inversions of solar data from reference models computed with temperature–optical depth relations obtained from the Eddington approximation and from the Harvard–Smithsonian Reference Atmosphere (Gingerich et al. 1971).

We have carried out additional comparisons. Some examples are illustrated in Fig. 10, in which both the reference model and the proxy Sun were obtained from the density distribution of model 2 beneath the photosphere, the sole difference being that the proxy had an atmosphere computed from the temperature–optical depth relation of the atmospheric model 5C of Vernazza, Avrett & Loeser (1981) and an opacity obtained by multiplying the values in the Cox–Tabor tables by a factor 1.5, intended to mimic the augmentation suggested by Cox (1990) resulting from a reassessment of the contribution from Fe. MHD5 was used to compute  $\gamma$ . Inversions using standard control parameters underestimate  $Y$  by  $3 \times 10^{-4}$  using method 1 and by  $1.1 \times 10^{-3}$  using method 2. These results, together with some others from inversions we have carried out using the reference models of Dziembowski et al. (1991), suggest that differences in the atmospheric models used by Däppen et al. (1991) and by Dziembowski et al. (1991) might account for no more than about 0.001 in the inferred value of  $Y$ . Of course, the solar atmosphere might be sufficiently different from those considered here, by virtue of its being laterally inhomogeneous and time dependent, that its misinterpretation introduces an error greater than this into the results of both methods.

#### 4.7 Internal stratification

The principal assumptions upon which the frequency constraints (1) depend are that the Sun and the reference model are both spherically symmetric and in hydrostatic balance,<sup>1</sup> and that their oscillation frequencies are well determined by linearized adiabatic theory. Of course, these assumptions are not satisfied in the very outer layers of the Sun but, as we have already argued, we hope to have eliminated most of the error arising from those layers by our use of

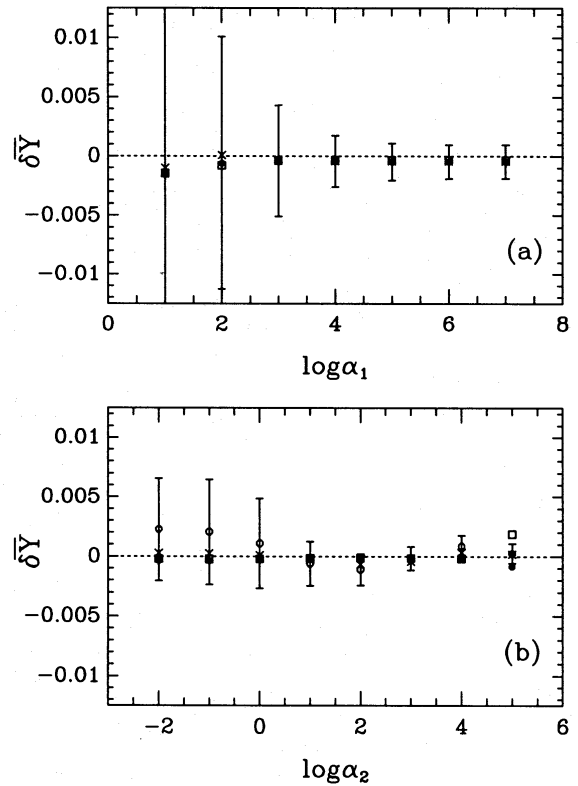


**Figure 10.** Inferred values of  $\delta Y$  for a sequence of inversions testing the influence of the atmospheric layers, for different values of  $\alpha_j$  and  $\Lambda_j$ . Reference solar model: model 2 computed with MHD5 and an atmosphere computed from the temperature–optical depth relation of the Harvard–Smithsonian Reference Atmosphere (Gingerich et al. 1971); proxy solar model: model 2 computed with MHD5 and an atmosphere computed from the temperature–optical depth relation from model 5C of Vernazza et al. (1981) with the opacity scaled by a factor of 1.5.  $Y_{\text{proxy}} = Y_{\text{ref}} = 0.2371$ . (a) Optimally localized averages with  $F(\nu_i) = 0$  (squares),  $\Lambda_1 = 3$  (full circles with error bars),  $\Lambda_1 = 7$  (crosses). (b) Least-squares inversions with  $F(\nu_i) = 0$  (squares),  $\Lambda_2 = 3$  (full circles),  $\Lambda_2 = 7$  (crosses),  $\Lambda_2 = 13$  (open circles with error bars).

$F(\nu)$  and, in method 1, also by explicit localization of the averaging kernels. In particular, no assumption is made about thermal balance, which suggests that the inversions should be insensitive to opacity and nuclear reaction rates. Furthermore, no assumption is made about the spatial variation of  $Y$ , nor how it came about, except that in method 2 the function  $Y$  is quite justifiably assumed to be constant throughout the region where  $\gamma$  varies substantially.

Explicit demonstrations of the role of thermal stratification and any variation of  $Y$  beneath the ionization zones are provided particularly by the inversions summarized in rows 1 and 11 in Table 2. The more extreme example is the chemically homogeneous model H. Although it was computed to be in thermal balance, its luminosity was deliber-

<sup>1</sup>More generally, it is required only that deviations from sphericity are small and that the averages of  $p$  and  $\rho$  over spherical surfaces satisfy the hydrostatic equations, provided that the multiplet frequencies  $\nu_i$  are regarded as uniformly weighted averages of the non-degenerate singlet frequencies over azimuthal order. Of course, it goes without saying that the mass and radius of the reference model must agree with those of the Sun (or the proxy model). However, the luminosities need not correspond.

ately set to only 90 per cent of the solar value to demonstrate the lack of sensitivity of the inversions to that parameter. As can be seen in Fig. 11, for the model the function  $u$  differs in places from that of the reference by as much as 24 per cent, particularly in the energy-generating core; the density differs by up to 40 per cent. Yet the determination of  $Y$  by method 1 is in error by no more than 0.003. Method 2 is rather less accurate in this case. (In the light of the discussion at the end of Section 4.1, that is not surprising; as is evident from Fig. 11, the function  $\delta u/u$  is not smooth near the base of the convection zone, and therefore the relatively large oscillatory average kernel  $A_{u,Y}$  illustrated in Fig. 1, introduces greater contamination of  $\delta \bar{Y}$  from errors in the hydrostatic structure.) Nevertheless, it must be borne in mind that the structure of model H, at least in the radiative interior, is known to differ from that of the Sun by much more than the structure of standard solar models (cf. Christensen-Dalsgaard, Gough & Thompson 1988b; Gough & Kosovichev 1988, 1990; Dziembowski et al. 1990; Christensen-Dalsgaard et al. 1991; Kosovichev & Fedorova 1991) such as reference models 2, 4 and R used for our inversions of solar data here. The inversions of model H should not, therefore, be considered to suggest that the estimations of the solar helium abundance recorded in rows 16–26 of Table 2 are less reliable by method 2 than they are by method 1. Model 4' has the wrong helium abundance  $Y(r)$  for its density stratification, and therefore is not in thermal balance if the opacity tables and the nuclear rates are to be believed; moreover its luminosity is also different from the solar value. Nevertheless, its helium abundance is still quite faithfully extracted by the inversion.

#### 4.8 Mode set

Däppen et al. (1991) used a smaller data set than did Dziembowski et al. (1991). The cost of optimally localized averaging increases with the number of modes much faster than that of method 2. Consequently attention was restricted to a

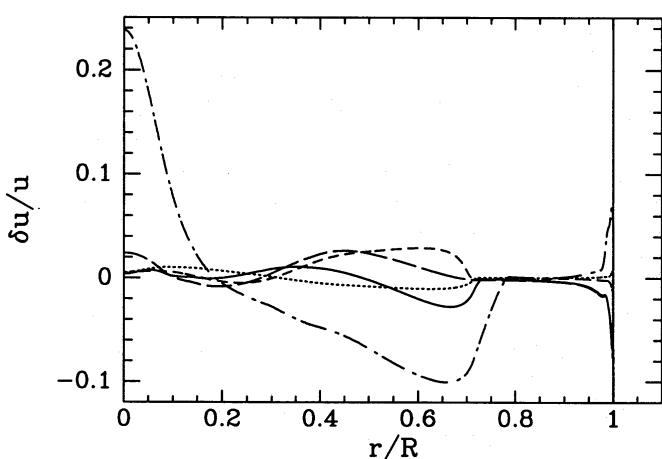


**Figure 11.** Relative differences  $\delta \ln u = \ln u - \ln u_2$  between the structure functions  $u = p/\rho$  of several of the proxy models and the corresponding function  $u_2$  of model 2, plotted against  $r/R$ , where  $R$  is the radius of the photosphere. The proxy models listed in Table 1 are model 4 (continuous curve), model 7 (dots), model 10 (short dashes), model 13 (long dashes) and model H (dot-dashed curve). The relative differences  $\delta \ln \rho$  in density tend to be larger; for example, for model H,  $\delta \ln \rho \approx 0.41$  at  $r=0$ .

subset of modes, namely modes with  $l \leq 140$  and  $\nu \leq 3$  mHz. With these are generally associated smaller observational errors, and they are less prone to influences from the uncertain outer layers of the Sun.

Some indication of the effect of changing the size of the mode set is provided by Dziembowski et al. (1991), who demonstrated in their fig. 4 essentially no influence on the value of  $Y$  from solar modes with  $l > 140$ . This is principally a consequence of the relatively low weighting given to those modes, resulting from their larger errors, and so does not provide quite the test of the method that Dziembowski et al. suspected.

It was the opinion of both Däppen et al. and Dziembowski et al. that one should avoid modes that are confined to the upper superadiabatic convective boundary layer. Otherwise, the inversions would be severely degraded by the uncertainties resulting from the substantial turbulent fluctuations that occur there. Däppen et al. chose to restrict attention to modes of relatively low frequency ( $\nu_i < 3$  mHz) whose upper turning points are quite deep, and whose frequencies are therefore relatively insensitive to the structure and dynamics of the boundary layer. Consequently, the inversion of the frequencies must also be insensitive to that layer. Dziembowski et al., on the other hand, argued that one should simply limit oneself to modes whose lower turning points are located well below  $\tau/T=0.9$  ( $r/R=0.997$ ). This level is safely below the boundary layer, yet above the region in which most of the effect of He ionization on  $\gamma$  occurs. The restriction is principally one on the degree  $l$  of the modes, and translates to requiring  $l/\nu$  to be substantially less than 180, where  $\nu$  is measured in mHz. By so doing, the uncertainties in frequency arising from the boundary layer are only weakly dependent on  $l$ , and their influence on the inversion should therefore be eliminated by the function  $F(\nu)$ .

An indication of how different modes contribute to the inversion is given by Fig. 12 in which we illustrate the coefficients  $c_i$ , plotted against the reduced frequency  $\nu/(l+\frac{1}{2})$  which determines the lower turning point. The magnitudes of the coefficients in panels (a) and (c) are determined to a great extent by the error estimates  $\sigma_i$ . However, if all the modes are weighted equally, assuming uniform standard errors equal to the mean of the observational estimates used for panels (a) and (c), the magnitudes of the coefficients are typically increased, particularly those which in reality have large  $\sigma_i$ . Consequently our estimate of the error in  $\bar{Y}$  is increased too. There is a tendency of modes with high  $l$  or high  $\nu$ , whose dynamics are more susceptible to the turbulent fluctuations in the upper convective boundary layer, to have the greater errors. It is these very modes that one would expect to be required to eliminate successfully the influence of the outer layers, particularly in method 1. Consequently, we would anticipate that by permitting them to have relatively greater weight an optimal inversion could be found with generally smaller values of  $c_i$ , which is not the case. We do not understand why that is so.

The predominant dependence of  $c_i$  on  $\sigma_i$  provides the explanation of the insensitivity of  $\bar{Y}$  to  $l_{\max}$  found by Dziembowski et al. (1991). Of course, the outcome of augmenting  $\mathcal{D}$  with modes of high frequency or high degree, when one uses artificial data computed from proxy solar models that are based on essentially the same physics as the reference, is not to alter substantially the value of  $Y$  inferred from inver-

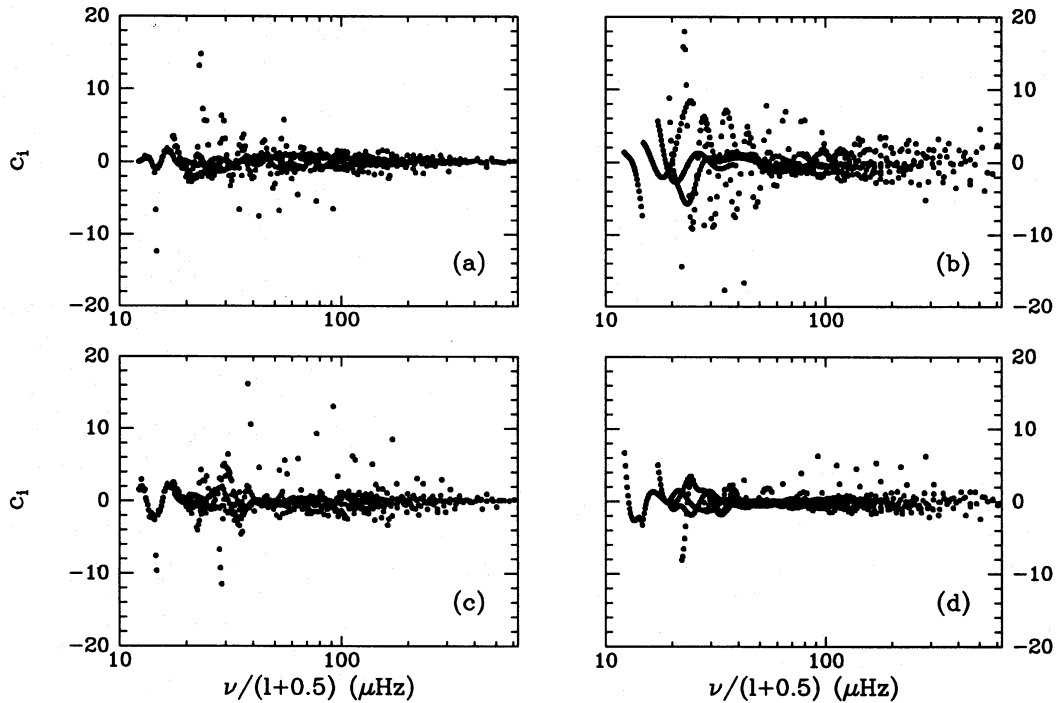


**Figure 12.** Coefficients  $c_i$  relating the averaging kernels  $A_{Y,u}$  to the data kernels  $K_{Y,u}^{(i)}$  according to equation (4): (a) determining optimally localized averages with  $\sigma_i$  appropriate to the observations of Libbrecht et al. (1990); (b) with uniform  $\sigma_i$ ; (c) from a least-squares inversion with  $\sigma_i$  appropriate to the observations; (d) with uniform  $\sigma_i$ . The reference is model 2, and standard control parameters have been used.

sions; it is merely to reduce the estimated random error, which is a natural consequence of using more data. However, when solar data are used, the outcome is different. Rows 27–29 of Table 2 record least-squares inversions of solar data using, respectively, modes of  $\mathcal{D}$  and all the modes published by Libbrecht et al. (1990), the latter being assigned first the observational error estimates and secondly equal values of  $\sigma_i$ . The first two inversions yield essentially the same results, as Dziembowski et al. (1991) found using the larger data sets that included the mean frequencies obtained by Jiménez et al. (1988) and the frequencies of high-degree modes ( $l > 140$ ) observed by Libbrecht et al. (1990) in 1987 by a technique different from that used for the intermediate-degree modes ( $l \leq 140$ ) in 1986. The reason is that the additional modes are given low weight by the large error estimates. When, in the third inversion, the weights are equalized, however, the results are significantly different: the estimate of  $\bar{Y}$  is increased by 0.036, yet the estimated error is only 0.003. Not only does this demonstrate the importance of the high-degree modes, but it also exposes once again the existence of a fundamental inconsistency between the theoretical and the solar frequencies that is not removed by  $F(\nu)$ .

#### 4.9 Equation of state

Both methods of determining  $Y$  require a precise knowledge of thermodynamic quantities, as functions not only of state variables but especially of the chemical composition. No laboratory data are available for the physical conditions in the solar convection zone, and we have therefore to rely on theoretical models of the plasma. These models are approximate realizations of the basic principles of statistical mechanics. In the simplest case, all particles in the plasma could be

considered to be non-interacting and without internal degrees of freedom, subject to reactions that describe the formation of ions and atoms and molecules. The maximum-entropy principle in the form of free-energy minimization yields the law of mass action in the form of the Saha equation, from which the equilibrium abundances of the species undergoing these reactions are obtained. This approximation is much too poor for our purposes. That has long been recognized, and has resulted in the use of substantially more sophisticated equations of state for helioseismic analyses (e.g. Berthomieu et al. 1980; Shibahashi, Noels & Gabriel 1983; Christensen-Dalsgaard, Däppen & Lebreton 1988a).

A first step away from the approximation of non-interacting particles is made by including the (classical) Coulomb potential between charged particles. Its influence is usually evaluated in the Debye–Hückel approximation, leading to a (negative) Coulomb-pressure correction. As a second step, one considers the internal degrees of freedom of the bound species. Here, there are two clearly distinct approaches, one being realized in the so-called chemical picture, the other in the physical picture (e.g. Däppen, Keady & Rogers 1991). While the chemical picture treats the bound systems as if they were independent particles (possibly with excited states), the physical picture deals only with fundamental particles (electrons and nuclei). The advantage of the chemical picture is that a wealth of results from atomic physics can be used, because the notion of atoms is still assumed to be valid, despite the plasma environment. Heuristic arguments have to be invoked to correct the atomic states for plasma effects, and only then can one proceed to the computation of the statistical mechanical equilibrium. The MHD equation of state follows this programme (Mihalas et al. 1988; Däppen et al. 1988b). In the physical picture there is no such separation. Here, the statistical mechanics is based on the Hamiltonian

governing the dynamics of the electrons and nuclei, and thus the bound systems are implicitly contained in the sum over all states of that Hamiltonian. The advantage of this procedure is that it tackles the statistical mechanics of the plasma at the same time as the quantum mechanics. In principle, no heuristic consideration about how the atoms and ions are perturbed by the surrounding plasma is therefore necessary. A practical realization of the physical picture has been pursued by a group at Livermore (Rogers 1986; Iglesias, Rogers & Wilson 1987). It turns out that a part of the (otherwise divergent) sum over bound states is taken away by terms in the continuum, which leads to the so-called Planck–Larkin partition function (whose main feature is that it essentially reduces the sum over bound states to include only those having a binding energy greater than  $kT$ ).

One might have thought that the thermodynamical quantities from the two approaches would differ from each other, perhaps by as much as they each differ from the simple Saha results. However, comparisons have shown that that is not the case (Däppen, Lebreton & Rogers 1990; Däppen 1990). A more careful analysis has shown that the most significant part of the deviation from the simple Saha result stems from the Coulomb–pressure correction, which has led to simplified equations of state that simulate well the features introduced by both the MHD and the Livermore equations of state (Christensen-Dalsgaard 1991). The similarity between the results of these approaches makes it more difficult to test the physics of the equation of state itself, because one has to find observable features that can still distinguish the small differences between the MHD and Livermore thermodynamic relations.

So far, we have discussed only the influence of hydrogen and helium. Although the signature of heavier elements has already been seen in the derivatives of  $\gamma$  (see Däppen & Gough 1984, 1986), it is weak, which is not surprising given that it arises basically in proportion to abundance by number. The first MHD tables for solar applications (Christensen-Dalsgaard et al. 1988a) were tailored to examine the effect on  $p$ -mode frequencies of details in the treatment of the hydrogen and helium ionization zones. To bypass prohibitive computations, savings were made in the treatment of the heavy elements. There are two ways to save: first, one can limit the number of heavy elements, while keeping their total mass fraction the same, and secondly, one has the option of neglecting the detailed partition functions of the bound states of a chosen number of ions of the heavy elements. Thus the amount of computation is controllable.

These practical considerations are the reason for the existence of different tables: in particular, MHD1 and MHD2. The MHD1 table was computed for the purposes of evolving solar models (Christensen-Dalsgaard et al. 1988a), and was therefore required to accommodate hydrogen burning in the core. For that study, the equation of state was computed without some of the partition functions of the higher ions of the heavy elements, with the idea in mind that it was prudent to represent a somewhat realistic chemical composition. The equation of state would thus be more consistent with the opacity used in the model, though this is hardly relevant in the convection zone. The MHD2 table, on the other hand, was computed for the He abundance calibration study of Däppen et al. (1988a), in which a comparison of solar envelope models was made. This investigation considered a

narrower range of physical conditions and, in particular, did not involve taking into account the comparatively wide variation of  $Y$  in the core. Therefore it was possible, with the resources available, to compute the tables on a finer mesh. MHD2 was used by Dziembowski et al. (1991) [and by Däppen et al. (1991) for the derivatives of  $\gamma$ , though the latter used reference models from Christensen-Dalsgaard et al. (1991), which were based on MHD1]. The differences between MHD1 and MHD2 were thought to be insignificant in the estimates of  $\gamma$  and its derivatives in the He II ionization zone.

It has now become clear that the detailed treatment of the heavy elements matters. Indeed, it has turned out that the choice of the number of heavy ions treated with detailed partition functions has an even stronger influence on  $\gamma$  than the selection of heavy elements in the chemical composition. To obtain a clearer picture, we have carried out MHD calculations for a test mixture that contains a mass fraction 0.02 of oxygen as the only heavy element. For a sequence of temperatures and densities corresponding to the second ionization zone of helium in the Sun, we have computed  $\gamma$ , and for each pair of temperature and density, we have systematically switched on (starting from the ground state) the full MHD partition functions. We did this first to neutral oxygen, then to  $O^+$ , then  $O^{++}$ , and finally to the hydrogenic ion. During this process, we have noted a variation of  $\gamma$  of a few parts in  $10^3$ , which at first sight is quite surprising given the small number of oxygen particles present (see also Däppen 1992). This can lead to an error in the inferred value of  $Y$  of several times greater magnitude.

To assess the importance of the approximations to the physics, we have augmented the MHD1 and MHD2 tables with three other tables. Their distinguishing characteristics are listed in Table 3. We have also added consistent partial derivatives of  $\gamma$  to MHD1, and all inversions from reference models with MHD1 reported in this paper were carried out with those consistent derivatives. Using both solar model 2 and solar model 4 as references, we have inverted the eigenfrequencies in  $\mathcal{D}$  of all the other models listed in Table 1 using all five versions of the equation of state in each of the proxy models. The entries in rows 2 to 6 of Table 2 typify the results. Versions 3–5 of the equation of state are rather similar and, when MHD5 is used for the reference, they yield the correct result typically to within about 5 parts in  $10^3$ ; with our standard control parameters, MHD2 produces an underestimate of about 0.008, and  $Y$  of the proxy with MHD1 is underestimated by nearly 0.025. An indication of how the estimates depend on the regularization parameters  $\alpha_j$  is given by Fig. 13. Notice that, when different equations of state are used in the reference and proxy models, stabilization with increasing  $\alpha_j$  tends to be slower. Notice also in Fig. 13(b) that, as  $\alpha_2$  becomes very large, the values of  $Y$  inferred from the least-squares inversion appear to be converging slowly towards the same value, which is close to the correct value, irrespective of the equation of state. (Of course, one cannot actually achieve that convergence by increasing  $\alpha_2$  yet further because, as is discussed in Section 4.2, at higher values of  $\alpha_2$  the solution is falsified by the excessive influence of the flatness constraint.) The optimal averages, on the other hand, converge to different values.

It follows from this study that, if the MHD equation of state with its treatment of excited states were indeed a rela-

**Table 3.** Equations of state.

Table	Composition <sup>a</sup>	Mesh size <sup>b</sup> : log $T$ / log $\rho$ / $Y$	Complete bound-state partition functions
MHD1	H, He, O, Fe	0.03/0.1/0.03	H, He, He <sup>+</sup> and neutral O and Fe only
MHD1'	H, He, O, Fe	0.09/0.3/0.03	H, He, He <sup>+</sup> and neutral O and Fe only
MHD2	H, He, O	0.03/0.1/0.03	all species
MHD3	H, He, C, N, O, Fe	0.03/0.1/0.03	H, He, He <sup>+</sup>
MHD4	H, He, C, N, O, Fe	0.03/0.1/0.03	all species of H, He, C, N, O, neutral Fe and Fe <sup>+</sup> only
MHD5	H, He, C, N, O, Fe	0.03/0.1/0.03	all species

Notes. <sup>a</sup>The relative abundances of O and Fe in MHD1 are 0.92 and 0.08. The relative abundances of C, N, O and Fe in MHD3–5 are 0.1776, 0.0433, 0.3926 and 0.3865, respectively;  $Z=0.02$ . <sup>b</sup>In all cases thermodynamic variables were obtained by four-point Lagrangian interpolation in log  $\rho$  and log  $T$  and quadratic interpolation in  $Y$ .

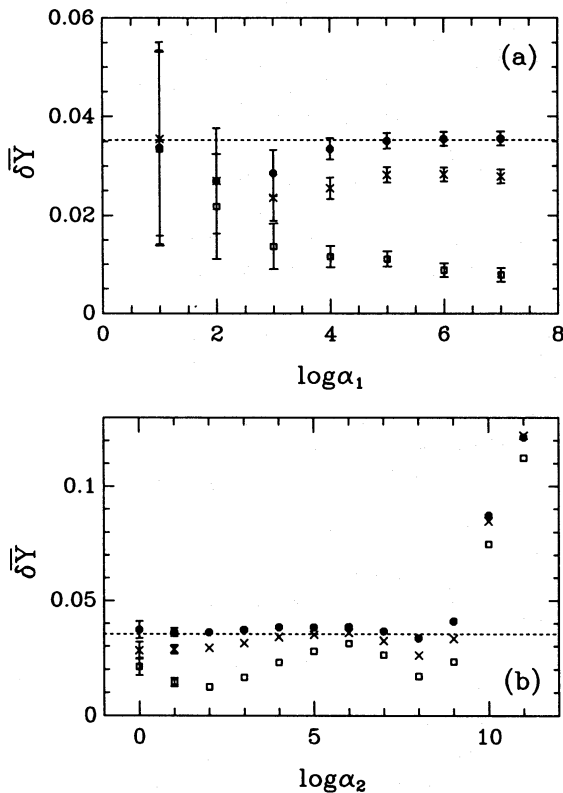


**Figure 13.** Inferred values of  $\delta Y$  for a sequence of inversions testing the influence of the equation of state. Reference solar model: model 2 ( $Y=0.2371$ ) with MHD5; proxy solar models: model 4 ( $Y=0.2724$ ) with MHD1 (squares), MHD2 (crosses) and MHD5 (circles). (a) Optimally localized averages ( $\Lambda_1=3$ ); (b) least-squares inversions ( $\Lambda_2=13$ ). Because of the large range of the ordinate, error bars are shown in (b) only for log  $\alpha_2=0$  and 1.

tively accurate description of reality, it could be concluded from hindsight that Dziembowski et al. (1991) happened to use a better set of tables (MHD2) than did Däppen et al. (1991). However, since the fundamental issues of the equation of state are not resolved yet, it is too early for a judgement. A collaboration with the Livermore group is

under way to ascertain whether an analogous effect results from the physical picture.

Finally, we point out that the major difference between the predictions of MHD1 and the other versions of the equation of state lies in the physical assumptions and not in interpolation error. We have tested this by recomputing models using a new MHD1 table on a finer grid. Inversions of model 2 with respect to itself computed with the finer tables are illustrated in Fig. 14, and show that the relative error introduced by interpolation is about 0.004 for method 1, and about 0.001 for method 2. Although, strictly speaking, this is not a direct test of using different reference models, the errors introduced are comparable, as is evidenced by comparing the inversions of row 6 of Table 2 with their reciprocal counterparts of row 12. We note also that the result of combining MHD2 partial derivatives of  $\gamma$  with MHD1 values of  $\gamma$  produces a false contribution of about 0.005 to the estimate of  $Y$  obtained by Däppen et al. (1991).

## 5 INVERSION OF SOLAR DATA

Several inversions of solar data have been carried out by the two methods. As in the work of Däppen et al. (1991), all the frequencies  $\nu_i$  and the estimated possible errors  $\sigma_i$  were taken from the observations of Libbrecht, Woodard and Kaufman, kindly supplied before publication (Libbrecht, Woodard & Kaufman 1990). Using the 1986 data reported by Libbrecht et al. (1990), we have varied  $\Lambda_j$ ,  $\alpha_j$ , the mode set and the reference model, to provide a comparison with the tests on artificial data. Some of the results are listed in Table 2.

The influence of  $\Lambda_j$  on  $\bar{Y}$  is similar to that found in Section 4: on the whole the inversions tend to stabilize as  $\Lambda_j$  increases. The dependence on  $\alpha_j$  is illustrated in Fig. 15, using three different versions of the equation of state for the reference models. The figure bears a superficial resemblance to Fig. 13. The optimal averages converge to constant values for  $\alpha_1 \gtrsim 10^4$ , the values depending on the version of the equation of state that was used for the reference model. Moreover, the differences between the values to which the optimal averages converge are more or less consistent with those found when inverting the artificial data (after taking



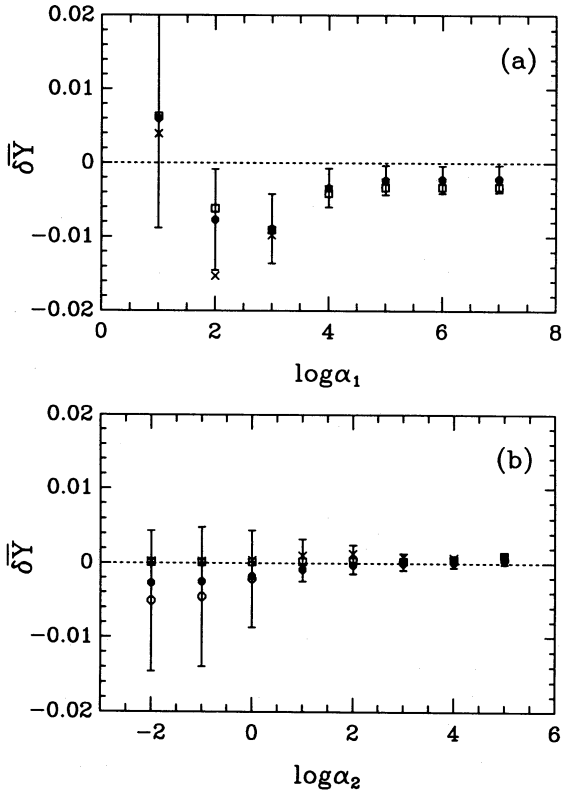


**Figure 14.** Inferred values of  $\delta Y$  for a sequence of inversions testing numerical errors in the equation of state, for different values of  $\alpha_j$  and  $\Lambda_j$ . Reference solar model: model 2, computed with fine MHD1 tables; proxy solar model: model 2, computed on the original coarser grid of the MHD1 tables. (a) Optimally localized averages with  $F(\nu_i)=0$  (squares),  $\Lambda_1=3$  (full circles with error bars),  $\Lambda_1=7$  (crosses); (b) least-squares inversions with  $F(\nu_i)=0$  (squares),  $\Lambda_2=3$  (full circles),  $\Lambda_2=7$  (crosses),  $\Lambda_2=13$  (open circles with error bars).

due account of the sign difference, because in Fig. 13 it is the equation of state of the proxy, not the reference, that varies). The inversions by least squares appear to be converging to the same value at very high  $\alpha_2$ , as in Fig. 13(b); the principal difference is that now none of the inversions seems to have converged fully, suggesting that all three sets of reference eigenfrequencies are inconsistent with the solar data.

We have also carried out comparable inversions of data from modes in  $\mathcal{D}$  obtained from observations by Libbrecht and Woodard in 1988 (private communication). Two examples are recorded in rows 21 and 26 of Table 2. Although the later frequencies are different from the 1986 data, and indicate a temporal variation in the structure of the Sun, particularly in the very outer layers, which is probably associated with the solar cycle (Libbrecht & Woodard 1990a, b), the helium abundance inferred from them is essentially unchanged. Therefore the inconsistency between the reference models and the Sun is unlikely to be related directly to whatever causes the solar cycle variation.

## 6 DISCUSSION

There exists a variety of procedures by which theoretical models of the Sun can be compared with observation in order to determine the abundance of helium in the solar interior. The superficially simplest is a straightforward

calibration of the models to the observed radius and luminosity at the presumed solar age,  $t_\odot$ , ignoring the seismic data. The calibration can be carried out for a wide range of chemical compositions and, if the composition is parameterized by the initial relative abundances  $X_0$ ,  $Y_0$  and  $Z_0=1-X_0-Y_0$  (presumed constant) of H,  ${}^4\text{He}$  and the aggregate of all other elements, it provides a unique relationship between  $Y_0$  and  $Z_0$ . Therefore, with some assumption about  $Z_0$ , which is typically (though sometimes implicitly) imposed as a value of  $Z_0/X_0$  obtained from observation (e.g. Anders & Grevesse 1989), a value of  $Y_0$  is obtained. One also obtains the helium abundance  $Y(r)$  at the present time. It is important to realize, however, that not only is the outcome dependent on the values of  $t_\odot$  and  $Z_0/X_0$  adopted, but it also depends on all the physics assumed in the construction of the solar models: the microscopic physics from which the opacity, the nuclear reaction rates and the equation of state are derived, and the macroscopic physics, which embodies all the ad hoc assumptions of the theory of stellar evolution. The calibration depends also on the initial conditions assumed. Thus the mere fact that the outcome appears now to be becoming robust, which Guenther et al. (1992) have recently emphasized, is hardly a reliable indication of the veracity of the conclusion.

A principal issue of concern is the macroscopic physics. For example, all standard solar models are unstable at some epochs in their evolution to thermally driven motion in the core (Christensen-Dalsgaard et al. 1974; Boury et al. 1975; Shibahashi, Osaki & Unno 1975; Saio 1980; Kosovichev & Severny 1985) and possible shear turbulence in the core and elsewhere (e.g. Zahn 1983). These instabilities are ignored in computing standard solar models. The models cannot, therefore, faithfully represent the Sun. The non-linear development of such instabilities is not adequately understood, and we do not know to what extent it modifies the solar structure. In particular, it could lead to a significant redistribution of helium (e.g. Dilke & Gough 1972; Schatzman et al. 1981; Roxburgh 1986; Ghosal & Spiegel 1991), and consequently degrade the calibration substantially. Helium settling against diffusion also modifies the overall structure (e.g. Cox, Guzik & Kidman 1989; Proffitt & Michaud 1991; Vauclair & Charbonnel 1991). The predominant modification it causes is in the outer layers of the radiative interior, which is largely compensated by an adjustment to the representation of the convection zone (via the mixing-length parameter). Therefore the influence on the value of  $Y_0$  is relatively small: Cox et al. (1989) found that settling could decrease the value of  $Y_0$  obtained from model calibration by about 0.002. The helium abundance in the convection zone might be reduced by as much as 0.05 (Vauclair & Charbonnel 1991; see also Guzik & Cox 1992; Proffitt & Michaud 1992).

Severe additional constraints are imposed by seismic data. In particular, accurate information about the sound speed throughout most of the solar interior has been provided by these data from which, for example, the location of the base of the adiabatically stratified region of the convection zone has been determined (Christensen-Dalsgaard et al. 1991). Such information could be used to constrain evolved solar models further. However, it cannot naively be added to the calibration without discarding one of the previously adopted constraints or assumptions, because the procedure would then be overdetermined.

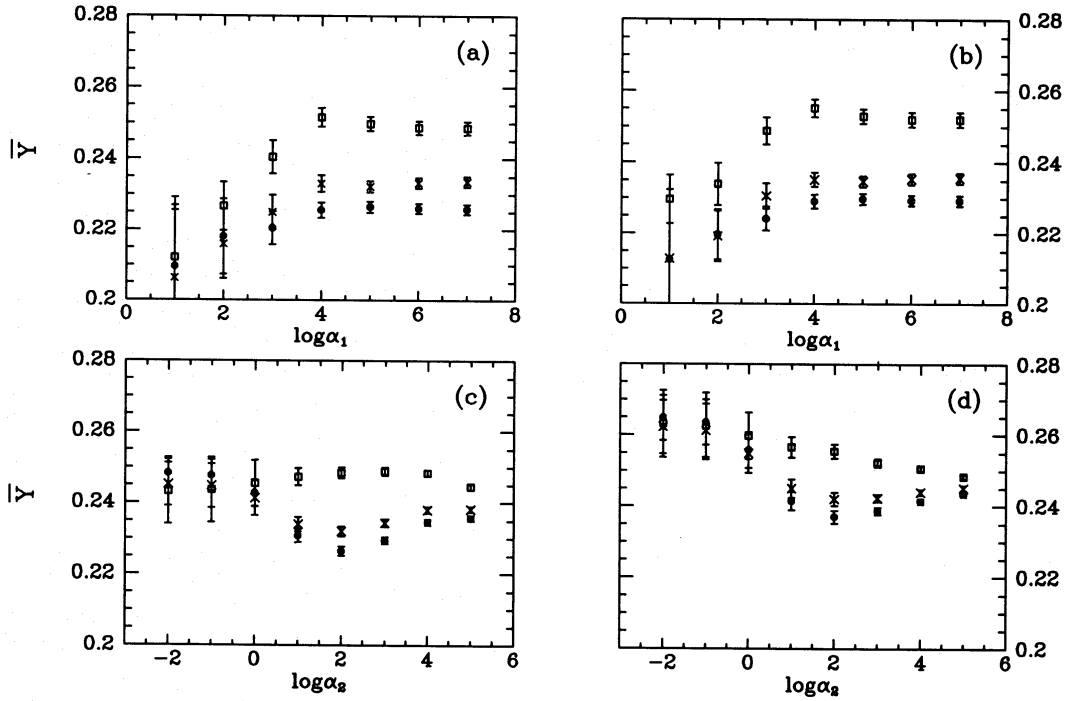


**Figure 15.** Inferred values  $\bar{Y}$  of  $Y$  for a sequence of inversions of solar frequencies measured by Libbrecht et al. (1990) obtained from two different reference models. Optimally localized averages (method 1) from (a) model 2 ( $Y=0.2371$ ) with MHD1 (squares), MHD2 (crosses) and MHD5 (circles), (b) model 4 ( $Y=0.2724$ ) with MHD1 (squares), MHD2 (crosses) and MHD5 (circles); least-squares inversions (method 2) from (c) model 2 ( $Y=0.2371$ ) with MHD1 (squares), MHD2 (crosses) and MHD5 (circles), (d) model 4 ( $Y=0.2724$ ) with MHD1 (squares), MHD2 (crosses) and MHD5 (circles). In all cases the standard regularization parameters ( $\alpha_1 = 10^4$ ,  $\beta = 1$ ,  $\Lambda_1 = 3$  for method 1;  $\alpha_2 = 10^2$ ,  $\Lambda_2 = 13$  for method 2) were used.

Of course, one possibility would be simply to vary  $Y_0$  to obtain a best fit of the eigenfrequencies of a sequence of theoretical models to the seismic data. Indeed, this is the first method to have been used to attempt to determine  $Y_0$  by seismic means (Christensen-Dalsgaard & Gough 1981). However, none of the theoretical models is consistent with observation, and a satisfactory fit cannot be obtained. Instead, the seismic data are revealing errors in the physics, such as in the calculations of opacity (Christensen-Dalsgaard et al. 1985; Iglesias & Rogers 1990, 1991; see also Korzenik & Ulrich 1989; Cox, Guzik & Raby 1990) and the treatment of the outer layers of the convection zone upon which the raw eigenfrequencies strongly depend, and which therefore degrade the calibration. In order to assess how best to carry out the calibration for any solar property such as  $Y$ , it is evidently essential to understand in what manner the eigenfrequency spectrum is influenced by different aspects of the Sun's structure (see Gough 1983), otherwise a discrepancy between theory and observations might be incorrectly interpreted. The situation is exemplified by the recent numerical studies by Guzik & Cox (1992), who reported some evidence that model convective envelopes having a helium abundance that is lower ( $Y \approx 0.24$ ) than the value of  $Y_0$  obtained from evolutionary models fit the (high degree) seismic data more closely, whereas Guenther et al. (1992) reported a Yale standard solar model without helium settling (with  $Y_0 = 0.28 \pm 0.01$ ) that reproduces the (low degree) oscillation spectrum within the errors associated with the uncertainties in the model physics.<sup>2</sup> This highlights the unreliability of the naive seismic model calibration.

Most of the modern seismic methods, however, are aimed

explicitly at obtaining the helium abundance  $Y$  directly. Since, except in the very surface layers, the oscillations are linear and adiabatic, they depend essentially only on the structure of the Sun through the hydrostatic stratification and the adiabatic exponent  $\gamma$ , and therefore they can sense  $Y$  only through  $\gamma$ . [Däppen et al. (1991) demonstrated that non-adiabatic effects and the effect of the modulation of the Reynolds stresses in the turbulent convection zone are successfully removed from the  $Y$  determination by method 1.] Consequently, it is only in the ionization zones of abundant elements that  $Y$  can be so determined. Of these, it is the second ionization zone of helium to which attention is normally directed. There, the macrophysics is relatively straightforward, and the influence of  $Y$  on  $\gamma$  is both direct and substantial. Of course, hydrogen also influences  $\gamma$  directly, indeed more so than helium, but it ionizes in the upper convective boundary layer in which the fluid dynamics is only poorly understood. The first ionization of helium is not well separated from that region. The ionization of other elements produces only a relatively small contribution to the variation of  $\gamma$ . However, we have discovered that the influence of trace elements on helium ionization cannot be ignored in the determination of  $Y$ .

It is evident that the principle of any direct seismic determination of  $Y$  must be to seek some combination of the data that is insensitive to the structure of all regions in the Sun except that in which the second ionization of helium occurs. To this end various schemes have been devised. The first was

<sup>2</sup>Moreover, Yale models into which helium settling has been introduced reproduce the seismic data less well (Pinsonneault 1992):

based on a determination of the sound speed  $c = (\gamma p / \rho)^{1/2}$  by inverse JWKB asymptotic analysis of high-degree modes, and comparing a feature of its functional form that is sensitive to  $Y$ , expressed in a function  $W(r)$ , with the results of similar analyses of the eigenfrequencies of a grid of solar envelope models (Däppen & Gough 1984, 1986; Däppen et al. 1988a). This method results from addressing explicitly the propagation of acoustic waves in the He II ionization zone. In so doing, it is necessary to eliminate from the frequencies a contribution that depends on the structure of the outer reflecting layers of the Sun. According to simple asymptotic theory, this can be accomplished because, unlike the influence of  $c$  on propagation, the influence of the outer layers essentially depends on frequency alone (e.g. Gough 1986). In practice, however, the contribution that is removed, which is usually represented in terms of a phase factor  $\tilde{\alpha}(\nu)$ , does not come solely from the reflecting layer. There is, in addition, an oscillatory component of  $\tilde{\alpha}$  which results from the breakdown of the asymptotic analysis in the He II ionization zone where the scale of variation of the background state is not small compared with the oscillation wavelength, and whose ‘period’ (about 0.7 mHz) is related directly to the acoustical depth of the zone (cf. Gough 1990). Added to this is a non-monotonic frequency-dependent contribution from the modulation of the turbulent convective fluxes (Gough 1984c; Balmforth 1992a,b). Thus the factor  $\tilde{\alpha}$  also contains information about helium ionization. Indeed, by comparing the solar  $\tilde{\alpha}$  with values of  $\tilde{\alpha}$  computed from a sequence of theoretical models (ignoring the turbulent fluxes), Christensen-Dalsgaard & Pérez Hernández (1991) and Vorontsov et al. (1991) have obtained values for  $Y$ . It is important to realize that, although the comparisons of both  $W$  and  $\tilde{\alpha}$  were motivated by asymptotic analysis, they do not depend directly on the accuracy of the asymptotics. They are strictly model calibrations based on eigenfrequencies that have been calculated numerically. The role of the asymptotic analysis is solely to provide a suitable procedure for processing the data to eliminate aspects that have no direct bearing on  $Y$ , and thereby to free the inferences from many of the errors resulting from the uncertain assumptions of the theory of stellar evolution.

The inversion procedures discussed in this paper are aimed at going even further towards removing unwanted components from the data. They depend only on the constraints (2), the only assumptions about the background state of the Sun contained within them being that it is in hydrostatic equilibrium with the observed mass and radius and that the stratification of its density and pressure is not far from that of the reference model, so that linearization is valid. (Strictly speaking, the second assumption would not be essential if the physics were well understood, because in that case the constraints could in principle be applied iteratively to provide a sequence of successively improved references.) The least-squares procedure for applying those constraints is basically a function-fitting operation, out of which, in the form in which it is used in method 2, the helium abundance emerges as a parameter. The procedure is driven by the requirement that the corrected model has eigenfrequencies consistent with observation, the particular model that is chosen having been selected by the regularization. The philosophy behind the optimal averages procedure (method 1) is quite different, for it is aimed directly at obtaining an average

of  $Y$  over a very narrow range of  $r$  rather than finding a new model that fits the data closely. In practice, however, the two methods are similar, and indeed both provide an average of  $Y$  as a linear combination (4) of the data, though, not surprisingly, the average from method 1 is more tightly confined to the desired region (see Figs 1a and c). In both methods the purpose of the regularization is to reduce contamination of the average by errors in the data, though that goal is sought explicitly only in method 1; in method 2 it is achieved implicitly by restricting the function space containing acceptable models, which here is based on the requirement that the difference between the reference model and the Sun is largely flat. Of course, the regularization in method 1 implicitly restricts the space of acceptable solutions also. However, neither regularization imposes the restrictions of the theory of stellar evolution, and therefore neither contaminates the measurement with the errors in the physics adopted by that theory.

We have tested the accuracy with which the two inversion methods are able to determine the helium abundance, at least under the condition that the reference model adequately incorporates the salient physics of mean hydrostatic support, and provided that adiabatic oscillation theory is sufficient to describe that aspect of the oscillations that is susceptible to changes in  $Y$ . By inverting artificial data with respect to the same reference models that we used for inverting solar data, we have shown that both methods can yield correct averages of  $Y$  in the convection zone, provided that the same equation of state was used for the proxy Sun and the reference model. It is important that both models are accurately in hydrostatic balance, but the details of the stratification are hardly relevant. It does not matter whether or not the luminosity of the reference model agrees with that of the proxy, nor whether or not the reference model is the outcome of a stellar evolution calculation. The procedures are thus completely insensitive to nuclear reaction rates and opacity, and therefore to whether or not the Sun is in thermal balance; they are insensitive also to the structure of the atmosphere, the distribution of helium in the core and, consequently, the presumed age of the Sun. Thus we arrive at the important practical corollary that it is unnecessary to have a theoretical model of the Sun that is computed from stellar evolution theory in order to measure the solar helium abundance. By concentrating on conditions solely in the region where helium ionizes, it is possible to divorce the measurement from any spurious properties elsewhere in the models, provided that the errors in those properties are small enough for linearization to be valid. Some indication of how far linear perturbation theory can be extended is provided by Fig. 9, which indicates that on the whole the salient aspects of the constraints (2) are valid even when the relative error in the reference value of  $Y$  is 25 per cent, and when, as can be seen from Fig. 11, the relative error in  $u$  is in some regions greater than 20 per cent (and the relative density error is as great as 50 per cent). Therefore, at present, iteration to a sequence of improved reference models is not necessary.

All direct seismological determinations of  $Y$  necessarily depend crucially on the equation of state. This is because the coefficients in the adiabatic wave equation are not determined completely by the hydrostatic stratification of the equilibrium model. They depend also on the sound speed  $c$ , which is related to  $p$  and  $\rho$  via the adiabatic exponent  $\gamma$ ,

upon which hydrostatic balance does not explicitly depend; the other quantities controlling the oscillations, namely the acoustic cut-off frequency and the buoyancy frequency, are then determined by  $c$  and the functions  $p$  and  $\rho$ . Indeed, it is the very existence of this independent function  $\gamma$  that permits  $Y$  to be determined. However, the transition from  $\gamma$  to  $Y$  is at present largely a product of theory. In this paper we have studied inversions with five versions of the equation of state; perusal of Table 2, and comparison of the entries with the inversions of solar data by Däppen et al. (1991) and Dziembowski et al. (1991), suggest that the major part of the discrepancy between the linearized estimates in the previously published inversions resulted from the use of different versions of the equation of state. It is difficult to state precisely how much of the discrepancy came about in this way, because, as we have confirmed by inverting artificial data from proxy models with different equations of state, the fundamental inconsistency that results interferes in a complicated way with other errors in the reference models; nevertheless, it is evident that the contribution to the discrepancy could have been as much as 0.03. A rather smaller contribution, about 0.005, resulted from numerical imprecision of the reference models used by Däppen et al. (1991) (see Christensen-Dalsgaard 1991), and a similar contribution resulted from the use of different data sets. [It is interesting to record, in passing, that Däppen et al. (1988a), who used the same version MHD2 of the equation of state as did Dziembowski et al. (1991), obtained  $Y=0.233 \pm 0.003$ , which is close to the value reported by Dziembowski et al. and to the corresponding solar values listed here in Table 2. Guzik & Cox (1992), from raw frequency calibrations, considered a similar low value of  $Y$  to be more nearly consistent with the data.] Almost all of the remaining difference has probably arisen from another fundamental inconsistency between the observations and the theoretical eigenfrequencies, which we have not isolated. Its presence, which was noticed in both the previous investigations, was accommodated by Dziembowski et al. with a non-linear adjustment downwards of typically 0.01 to the linearized estimates  $\delta\bar{Y}$  of  $\delta Y$ . The procedure for making that adjustment, under the assumption that  $\delta\bar{Y}$  vanishes with  $\delta Y$ , is itself uncertain by as much as about 0.01, as we have shown in Section 4.6. However, as we have demonstrated also in Section 4.6, that inconsistency has not arisen merely from errors in parameters, such as  $Y$  itself, defining the reference models, as Dziembowski et al. originally believed, since proxy models computed with  $Y$  that seem to deviate from the reference by rather more than does the Sun maintain the linear law. It appears, therefore, that the inconsistency arises either from some serious flaw in the physics assumed in the computation of the reference models or from systematic observational error.

If the error were in the physics, where could it be? Perhaps the most obvious possibility is in the equation of state.<sup>3</sup> We have found a considerable variation in the value of  $Y$  inferred from artificial seismic data as the relative abundances of heavy elements in the proxy model are varied at fixed  $Z$ . Varying the composition of the reference for a fixed

proxy, which is a more direct analogue of the solar inversions, produces similar results; we have not carried out such extensive comparisons of that kind, however, because it is computationally much more expensive. What is, at first sight, surprising about these results, however, is the high sensitivity of the outcome of the inversions to the relative heavy-element abundances, for their ionization in the He II ionization zone produces only a small contribution to the thermodynamic function  $p(\rho, T, X_k)$ . The reason for the sensitivity is that the inversion, which is based not only on the value of  $\gamma$  but also on its variation, depends principally on derivatives of the thermodynamic function, which is a more delicate product of the theory. In this investigation we have confined attention to the MHD formulation, which is one of the best, though not necessarily the best, formulation available. And, naturally, we have put the most emphasis on the most complete version of it, namely MHD5. However, MHD5 may not actually have been the most accurate. Indeed, detailed (unpublished) comparisons of  $\gamma$  and its derivatives produced by MHD and by the recent calculations of Iglesias & Rogers (see Däppen 1992) reveal what might be significant differences: in some respects, the equation of state of Iglesias & Rogers, for the composition of MHD5, is more similar to MHD1 (in which the ions of the heavy elements were assumed to be in the ground states) than it is to MHD5, a result which might have been expected intuitively from the form of the Plank–Larkin partition function.

Another possible source of error is in the treatment of the outer layers of the Sun. Non-adiabatic processes and Reynolds stresses make significant modifications to the eigenfrequencies (Christensen-Dalsgaard & Frandsen 1983; Gough 1984c; Cox et al. 1989; Balmforth 1992a, b). The direct influence of horizontal inhomogeneity in the upper convective boundary layer is also substantial (cf. Brown 1984). However, like the non-adiabatic processes and the influence of Reynolds stresses, it should have been largely eliminated by the use of  $F(\nu)$ , either explicitly in equation (12) used by method 2 or via the constraints (10) imposed in method 1. Nevertheless, it is not out of the question that, by misrepresenting the outer layers, an erroneous relation between, say, the displacement eigenfunction and the pressure fluctuation could have corrupted the kernels by so much that they have not been successful in producing a combination of the data that correctly determines  $Y$ . However, the evidence provided by tests with real and artificial data reported in this and the earlier papers does at least suggest that the corruption is not serious.

An interesting difference between the responses of the two inversion methods to errors in physics is evident in Fig. 13. When different equations of state are used for the reference and proxy models, the optimally localized averages, which concentrate on conditions in the He II ionization zone, yield erroneous estimates of  $Y$ , as should be expected. However, the results of method 2 seem to be approaching the correct value as the regularization parameter  $a_2$  increases, irrespective of the reference equation of state. It appears that, as the degree of regularization is increased, forcing the solution  $u(x)$  to be closer to the reference and yielding broader averaging kernels for  $Y$ , the local errors in the equation of state where He is undergoing its second ionization are first partially cancelled by compensating errors from elsewhere. However, that trend does not continue indefinitely. When  $a_2$

<sup>3</sup>Subsequent to this analysis, Dziembowski, Pamyanykh & Sienkiewicz (1992) have reported further on the inconsistency of MHD2 with the data.

is increased beyond  $10^6$ , contamination from the errors in  $u$  dominate, and the inferred values of  $Y$  diverge.

Finally, we comment on the value of the solar  $Y$ . As we have already noted, the inversions of solar data illustrated in Fig. 15 bear a qualitative resemblance to those in Fig. 13. In particular, the confluence of the least-squares inversions from different equations of state as  $\alpha_2$  increases is again exhibited. However, it must be realized that the nature of the inconsistency between the solar data and the eigenfrequencies of the reference model might be quite different from that resulting from our use of different MHD formulations of the equation of state, and therefore the confluence of the inversions could be misleading. For this reason, we refrain from conjecturing on the magnitude of the uncertainty in the estimates of the value of  $Y$ .

## 7 CONCLUSIONS

We have compared properties of the methods that Däppen et al. (1991) and Dziembowski et al. (1991) used to infer the helium abundance  $Y$  in the solar convection zone. Both methods are based on an inversion of linearized integral constraints (2) imposed by the differences between solar  $p$ -mode frequencies and the eigenfrequencies of theoretical reference models of the Sun. When, using the same reference model, the two methods are each applied to the same artificial data obtained from another theoretical solar model computed with the same equation of state as that used for the reference, there seems to be little to choose between the results. Some examples can readily be compared in Table 2 and Fig. 9. One can also judge from Fig. 9 the accuracy of the linearization leading to equation (2). In particular, there is little justification for the non-linear modification that Dziembowski et al. made to their linear estimates. This modification was responsible for a substantial fraction of the difference between the published abundance determinations. A similar contribution to the difference came from a combination of a small error in the computation of hydrostatic support in the reference models used by Däppen et al., which we have now corrected, and an inconsistency between  $\gamma$  and its partial derivatives with respect to  $p$ ,  $\rho$  and  $Y$ . The use of different mode sets appears to have contributed negligibly to the discrepancy.

The principal difference, however, between the estimates of the solar  $Y$  obtained by Däppen et al. and Dziembowski et al. results from their use of different equations of state in the reference models. Both equations were based on the MHD formulation, but they differed in the approximate treatments of the heavy elements. We have now computed new tables in which the heavy elements are treated consistently within the MHD formalism, and we have compared their seismic properties with the earlier versions; the version that had been used by Dziembowski et al. is the closer.

When inconsistent data are used, such as eigenfrequencies of a model computed with a different equation of state from that used for the reference model, the two methods respond somewhat differently. We cannot judge from the inversions alone which method is the more accurate.

Within the framework of standard solar theory, it is only hydrostatic support and the equation of state that need to be represented accurately by the reference model, particularly if optimally localized averaging is used. The reference model

must have the correct solar mass and radius, but it need not have the correct luminosity, nor be the product of an evolution calculation. The details of the hydrostatic stratification are hardly relevant, however; what really matters is simply that the hydrostatic equation be satisfied. This is exemplified by the use of a chemically homogeneous model for the reference, through which the distributions of density and sound speed are rather different from those in the Sun. As can be seen in Table 2, both inversion methods recover the helium abundance in the convection zone of a proxy model reasonably well, the error in the optimally localized average being only 0.003. Thus the inversions are not susceptible to most of the uncertain assumptions of stellar evolution theory, nor to the values of the nuclear reaction rates and opacity upon which the calibration of standard solar models crucially depends.

Inversions using the best of our equations of state cannot be made to explain the solar data to the same precision as they do the eigenfrequencies of theoretical models computed using the same physics. The residual discrepancy could be observational error or an error in the physics of the reference model, such as the equation of state. Inversions such as those listed in Table 2 suggest a value for the helium abundance  $Y$  in the solar convection zone of approximately  $0.232 \pm 0.006$ . The uncertainty is formal and was estimated from the spread in results obtained by the different methods using various reference models, ignoring the last entry in Table 2. It takes no account of the systematic errors resulting from misrepresenting the physics in the reference model, and particularly from errors in the equation of state. Until an understanding of those errors is established, the true reliability of the estimate cannot be judged.

## ACKNOWLEDGMENTS

We are very grateful to K. G. Libbrecht for supplying solar data prior to publication. We thank A. N. Cox for commenting, as referee, on the original submitted version of this paper. The work reported in the paper was carried out partly at the Institute for Theoretical Physics of the University of California at Santa Barbara, which is supported by the National Science Foundation under grant PHY89-04035 supplemented by funds from the National Aeronautics and Space Administration. Support from the UK Science and Engineering Research Council, the USSR Academy of Sciences, the Danish Natural Science Research Council and the Danish Space Board is gratefully acknowledged.

## REFERENCES

- Anders, E. & Grevesse, N., 1989. *Geochim. Cosmochim. Acta*, **53**, 197.
- Backus, G. & Gilbert, F., 1968. *Geophys. J. R. Astron. Soc.*, **16**, 169.
- Backus, G. & Gilbert, F., 1970. *Phil. Trans. R. Soc. London. A*, **266**, 123.
- Bahcall, J. N. & Ulrich, R. K., 1988. *Rev. Mod. Phys.*, **60**, 297.
- Balmforth, N. J., 1992a. *Mon. Not. R. Astron. Soc.*, **255**, 603.
- Balmforth, N. J., 1992b. *Mon. Not. R. Astron. Soc.*, **255**, 632.
- Berthomieu, G., Cooper, A. J., Gough, D. O., Osaki, Y., Provost, J. & Rocca, A., 1980. In: *Nonradial and nonlinear stellar pulsations*, p. 307, eds Hill, H. A. & Dziembowski, W. A., Springer, Heidelberg.

- Boury A., Gabriel, M., Noels, A., Scuflaire, R. & Ledoux, P., 1975. *Astron. Astrophys.*, **41**, 279.
- Brown, T. M., 1984. *Science*, **226**, 687.
- Christensen-Dalsgaard, J., 1988. In: *Seismology of the sun and sun-like stars*, p. 431, ed. Rolfe, E. J., ESA SP-286, Noordwijk.
- Christensen-Dalsgaard, J., 1991. In: *Challenges to theories of the structure of moderate-mass stars*, p. 11, eds Gough, D. O. & Toomre, J., Springer, Heidelberg.
- Christensen-Dalsgaard, J. & Frandsen, S., 1983. *Solar Phys.*, **83**, 165.
- Christensen-Dalsgaard, J. & Gough, D. O., 1981. *Astron. Astrophys.*, **104**, 173.
- Christensen-Dalsgaard, J. & Pérez Hernández, F., 1991. In: *Challenges to theories of the structure of moderate-mass stars*, p. 43, eds Gough, D. O. & Toomre, J., Springer, Heidelberg.
- Christensen-Dalsgaard, J., Dilke, F. W. W. & Gough, D. O., 1974. *Mon. Not. R. Astron. Soc.*, **169**, 429.
- Christensen-Dalsgaard, J., Däppen, W. & Lebreton, Y., 1988a. *Nature*, **336**, 634.
- Christensen-Dalsgaard, J., Gough, D. O. & Thompson, M. J., 1988b. In: *Seismology of the sun and sun-like stars*, p. 457, ed. Rolfe, E. J., ESA SP-286, Noordwijk.
- Christensen-Dalsgaard, J., Gough, D. O. & Thompson, M. J., 1991. *Astrophys. J.*, **378**, 413.
- Christensen-Dalsgaard, J., Duvall, T., Jr, Gough, D. O., Harvey J. W. & Rhodes, E. J., Jr, 1985. *Nature*, **315**, 378.
- Cooper, A. J., 1981. *PhD thesis*, Cambridge University.
- Cox, A. N., 1990. In: *Inside the sun, IAU Colloq. No. 121*, p. 61, eds Berthomieu, G. & Cribier, M., Kluwer, Dordrecht.
- Cox, A. N. & Tabor, J. E., 1976. *Astrophys. J. Suppl.*, **31**, 271.
- Cox, A. N., Guzik, J. A. & Kidman, R. B., 1989. *Astrophys. J.*, **342**, 1187.
- Cox, A. N., Guzik, J. A. & Raby, S., 1990. *Astrophys. J.*, **353**, 698.
- Däppen, W., 1990. In: *Progress of seismology of the sun and stars*, p. 33, eds Osaki, Y. & Shibahashi, H., Springer, Berlin.
- Däppen, W., 1992. *Rev. Mex. Astron. Astrofis.*, **23**, 141.
- Däppen, W. & Gough, D. O., 1984. In: *Theoretical problems in stellar stability and oscillations*, p. 264, eds Noels, A. & Gabriel, M., Proc. 25th Liège Int. Astrophys. Colloq., Inst. d'Astrophys., Univ. de Liège.
- Däppen, W. & Gough, D. O., 1986. In: *Seismology of the sun and the distant stars, NATO ASI Ser. C.*, Vol. 169, p. 275, ed. Gough D. O., Reidel, Dordrecht.
- Däppen, W., Gough, D. O. & Thompson, M. J., 1988a. In: *Seismology of the sun and sun-like stars*, p. 505, ed. Rolfe, E. J., ESA SP-286, Noordwijk.
- Däppen, W., Mihalas, D., Hummer, D. G. & Mihalas, B. W., 1988b. *Astrophys. J.*, **332**, 261.
- Däppen, W., Lebreton, Y. & Rogers, F. J., 1990. *Solar Phys.*, **128**, 35.
- Däppen, W., Keady, J. & Rogers, F., 1991. In: *Solar interior and atmosphere*, p. 112, eds Cox, A. N., Livingston, W. C. & Matthews, M. S., Univ. Arizona Press, Tucson.
- Däppen, W., Gough, D. O., Kosovichev, A. G. & Thompson, M. J., 1991. In: *Challenges to theories of the structure of moderate-mass stars*, p. 111, eds Gough, D. O. & Toomre, J., Springer, Heidelberg.
- Dilke, F. W. W. & Gough, D. O., 1972. *Nature*, **240**, 262, 293.
- Dziembowski, W. A., Pamyatnykh, A. A. & Sienkiewicz, R., 1990. *Mon. Not. R. Astron. Soc.*, **244**, 542.
- Dziembowski, W. A., Pamyatnykh, A. A. & Sienkiewicz, R., 1991. *Mon. Not. R. Astron. Soc.*, **249**, 602.
- Dziembowski, W. A., Pamyatnykh, A. A. & Sienkiewicz, R., 1992. *Acta Astron.*, **22**, 5.
- Fowler, W. A., Caughlan, G. R. & Zimmerman, B. A., 1975. *Ann. Rev. Astron. Astrophys.*, **13**, 69.
- Ghosal, S. & Spiegel, E. A., 1991. *Geophys. Astrophys. Fluid Dynamics*, **61**, 161.
- Gingerich, O., Noyes, R. W., Kalkofen, W. & Cuny, Y., 1971. *Solar Phys.*, **18**, 347.
- Gough, D. O., 1983. In: *Primordial Helium*, p. 117, eds Shaver, P. A., Kunth, D. & Kjær, K., European Southern Observatory, Garching.
- Gough, D. O., 1984a. *Mem. Soc. Astron. Ital.*, **55**, 13.
- Gough, D. O., 1984b. In: *Solar seismology from space*, p. 49, eds Ulrich, R. K., Harvey, J. W., Rhodes, E. J., Jr & Toomre, J., Pasadena. Jet Propulsion Laboratory.
- Gough, D. O., 1984c. *Adv. Space Res.*, **4**, No. 8, 85.
- Gough, D. O., 1986. In: *Seismology of the sun and the distant stars, NATO ASI Ser. C.*, Vol. 169, p. 125, ed. Gough, D. O., Reidel, Dordrecht.
- Gough, D. O., 1990. In: *Progress of seismology of the sun and stars*, p. 283, eds Osaki, Y. & Shibahashi, H., Springer, Heidelberg.
- Gough, D. O., 1992. In: *Astrophysical Fluid Dynamics, Proc. Les Houches Session XLVII*, North Holland, Amsterdam, in press.
- Gough, D. O. & Kosovichev, A. G., 1988. In: *Seismology of the sun and sun-like stars*, p. 195, ed. Rolfe, E. J., ESA SP-286, Noordwijk.
- Gough, D. O. & Kosovichev, A. G., 1990. In: *Inside the Sun*, p. 327, eds Berthomieu, G. & Cribier, M., Kluwer, Dordrecht.
- Gough, D. O. & Toomre, J., 1990. *GONG Newsletter* (National Solar Observatory, Tucson), **14**, p. 16.
- Gough, D. O. & Thompson, M. J., 1991. In: *Solar interior and atmosphere*, p. 519, eds Cox, A. N., Livingston, W. C. & Matthews, M. S., Univ. Arizona Press, Tucson.
- Guenther, D. B., Demarque, P., Kim, Y.-C. & Pinsonneault, M. H., 1992. *Astrophys. J.*, **387**, 372.
- Guzik, J. A. & Cox, A. N., 1992. *Astrophys. J.*, **386**, 729.
- Huebner, W. F., Merth, A. L., Magee, N. H. & Argo, M. F., 1977. *Astrophysical Opacity Library*, Los Alamos Scientific Laboratory, Report LA - 6760-M (LAOL).
- Hummer, D. G. & Mihalas, D., 1988. *Astrophys. J.*, **331**, 794.
- Iglesias, C. A. & Rogers, F. J., 1990. In: *Inside the sun*, p. 81, eds Berthomieu, G. & Cribier, M., Kluwer, Dordrecht.
- Iglesias, C. A. & Rogers, F. J., 1991. *Astrophys. J. Lett.*, **371**, L73.
- Iglesias, C. A., Rogers, F. J. & Wilson, B., 1987. *Astrophys. J. Lett.*, **322**, L45.
- Jiménez, A., Pallé, P. L., Pérez, J. C., Régulo, C., Roca Cortés, T., Isaak, G. R., McLeod, C. P. & van der Raay, H. B., 1988. In: *Advances in helio- and asteroseismology, IAU Symp. No. 123*, p. 205, eds Christensen-Dalsgaard, J. & Frandsen, S., Reidel, Dordrecht.
- Korzennik, S. G. & Ulrich, R. K., 1989. *Astrophys. J.*, **339**, 1144.
- Kosovichev, A. G. & Severny, A. B., 1985. *Izv. Krymsk. Astrofiz. Obs.*, **72**, 188.
- Kosovichev, A. G. & Fedorova, A. V., 1991. *Soviet Astron.*, **35** (5), 507.
- Libbrecht, K. G. & Woodard, M. F., 1990a. In: *Progress of seismology of the sun and stars*, p. 145, eds Osaki, Y. & Shibahashi, H., Springer, Heidelberg.
- Libbrecht, K. G. & Woodard, M. F., 1990b. *Nature*, **345**, 779.
- Libbrecht, K. G., Woodard, M. F. & Kaufman, J. M., 1990. *Astrophys. J. Suppl.*, **74**, 1129.
- Mihalas, D., Däppen, W. & Hummer, D. G., 1988. *Astrophys. J.*, **331**, 815.
- Parker, P. D., 1986. In: *Physics of the sun*, Vol. 1, p. 15, eds Sturrock, P. A., Holtzer, T. E., Mihalas, D. & Ulrich, R. K., Reidel, Dordrecht.
- Phillips, D. L., 1962. *J. Assoc. Comput. Mach.*, **9**, 84.
- Pinsonneault, M., 1992. In: *Massive neutrinos: tests of fundamental symmetries*, ed. Tran, T. V., Editions Frontières, Gif sur Yvette, in press.
- Proffitt, C. R. & Michaud, G., 1991. *Astrophys. J.*, **371**, 584.
- Proffitt, C. R. & Michaud, G., 1992. In: *Inside the stars*, eds Baglin, A. & Weiss, W., in press.
- Rogers, F. J., 1986. *Astrophys. J.*, **310**, 723.

- Roxburgh, I. W., 1986. In: *Seismology of the sun and the distant stars*, NATO ASI Ser. C, Vol. 169, p. 265, ed. Gough, D. O., Reidel, Dordrecht.
- Saio, H., 1980. *Astrophys. J.*, **240**, 685.
- Schatzman, E., Maeder, A., Angrand, F. & Glowinski, R., 1981. *Astron. Astrophys.*, **96**, 1.
- Shibahashi, H., Osaki, Y. & Unno, W., 1975. *Publs Astron. Soc.*, **27**, 401.
- Shibahashi, H., Noels, A. & Gabriel, M., 1983. *Astron. Astrophys.*, **123**, 283.
- Thompson, M. J., 1991. In: *Challenges to theories of the structure of moderate-mass stars*, p. 61, eds Gough, D. O. & Toomre, J., Springer, Heidelberg.
- Tikhonov, A. N. & Arsenin, V. Y., 1977. *Solution of ill-posed problems*, Winston, Washington, DC.
- Unno, W., Osaki, Y., Ando, H., Saio, H. & Shibahashi, H., 1989. *Nonradial oscillations of stars*, Univ. Tokyo Press, Tokyo.
- Vauclair, S. & Charbonnel, C., 1991. In: *Challenges to theories of the structure of moderate-mass stars*, p. 37, eds Gough, D. O. & Toomre, J., Springer, Heidelberg.
- Vernazza, J. E., Avrett, E. H. & Loeser, R., 1981. *Astrophys. J. Suppl.*, **45**, 635.
- Vorontsov, S. V., Baturin, V. A. & Pamyatnykh, A. A., 1991. *Nature*, **349**, 49.
- Zahn, J. P., 1983. In: *Astrophysical processes in upper main sequence stars*, p. 253, eds Hauck, B. & Maeder, A., Geneva Observatory, Sauveny.